Proteomic and metabolomic approaches unveil relevant biochemical changes in carbohydrate and cell wall metabolisms of two blueberry (*Vaccinium corymbosum*) varieties with different quality attributes

M.L. Montecchiarini, E. Margarit, L. Morales, M.F. Rivadeneira, F. Bello, A. Gollán, D. Vázquez, F.E. Podestá, K.E.J. Tripodi

PII: S0981-9428(18)30566-7

DOI: https://doi.org/10.1016/j.plaphy.2018.12.019

Reference: PLAPHY 5539

To appear in: *Plant Physiology and Biochemistry*

Received Date: 16 October 2018

Revised Date: 13 December 2018

Accepted Date: 19 December 2018

Please cite this article as: M.L. Montecchiarini, E. Margarit, L. Morales, M.F. Rivadeneira, F. Bello, A. Gollán, D. Vázquez, F.E. Podestá, K.E.J. Tripodi, Proteomic and metabolomic approaches unveil relevant biochemical changes in carbohydrate and cell wall metabolisms of two blueberry (*Vaccinium corymbosum*) varieties with different quality attributes, *Plant Physiology et Biochemistry* (2019), doi: https://doi.org/10.1016/j.plaphy.2018.12.019.

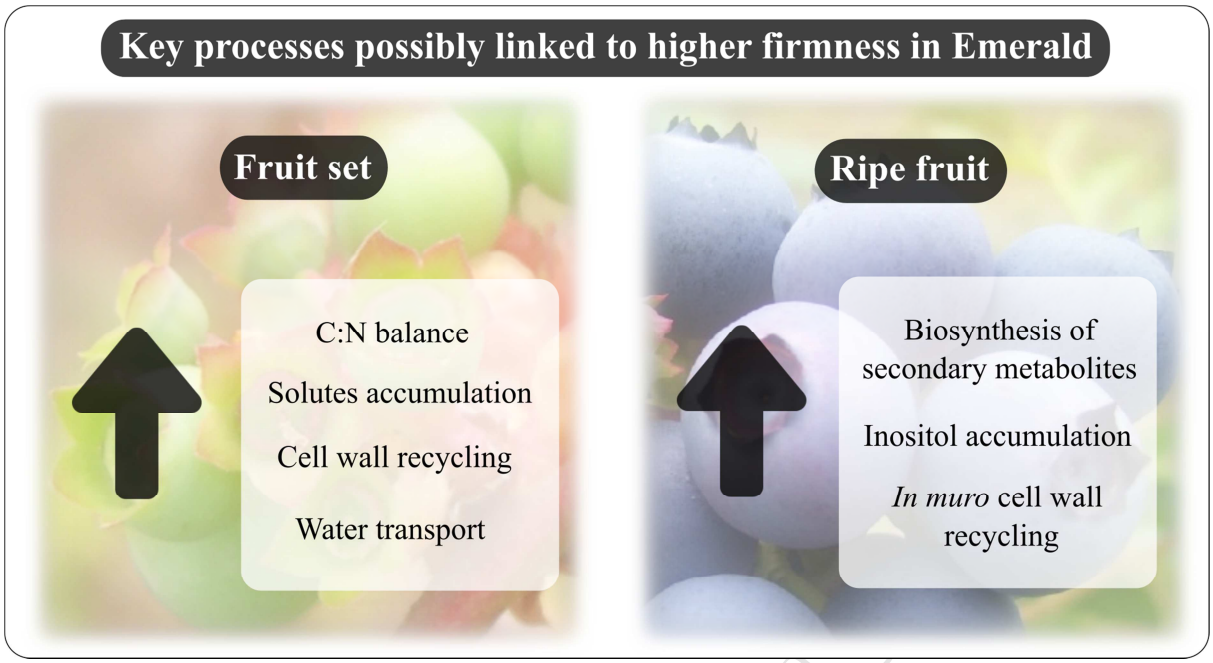

Proteomic and metabolomic approaches unveil relevant biochemical changes in carbohydrate and cell wall metabolisms of two blueberry (*Vaccinium corymbosum*) varieties with different quality attributes

Montecchiarini, M.L.[a]; Margarit, E.[a]; Morales, L.[a], Rivadeneira, M.F.[b]; Bello; F.[b], Gollán, A.[b], Vázquez, D.[b]; Podestá[a], F. E.[a]* and Tripodi, K.E.J.[a]*

[a] Centro de Estudios Fotosintéticos y Bioquímicos (CEFOBI), Facultad de Ciencias Bioquímicas y Farmacéuticas, Universidad Nacional de Rosario, Suipacha 531, 2000, Rosario (Santa Fe), Argentina

[b] Estación Experimental Concordia, Instituto Nacional de Tecnología Agropecuaria (INTA), Estación Yuquerí, 3200, Concordia (Entre Ríos), Argentina.

* Corresponding authors email: tripodi@cefobi-conicet.gov.ar, podesta@cefobi-conicet.gov.ar

Research paper

Abstract

Quality maintenance in rapidly decaying fruit such as blueberries (*Vaccinium corymbosum*) is of essential importance to guarantee the economic success of the crop. Fruit quality is a multifaceted subject that encompasses flavor, aroma, visual and physical issues as main factors. In this paper we report an ample characterization of different biochemical and physical aspects in two varieties (O´Neal and Emerald) of blueberries that differ in firmness, aspect, flavor and harvesting times, at two different phenological stages (fruit set vs. ripe), with the intention of unveiling how the metabolic signature of each contributes to their contrasting quality. To this effect a metabolomic, ionomic and proteomic approach was selected. The results presented here show marked differences in several variables at the two stages and between varieties. Emerald is an early variety with a large, good taste and firm fruit, while O'Neal is soft, medium sized and very sweet. Proteomic data comparison between both cultivars showed that, at fruit set, processes related with the response to inorganic compounds and small molecule metabolisms are relevant in both varieties. However, solute accumulation (mainly amino acids and organic acids), enzymes related with C: N balance, water transport and cell wall recycling are enhanced in Emerald. In ripe fruit, Emerald showed an enrichment of proteins associated with TCA, nitrogen, small molecules and cell wall *in muro* recycling processes, while mannitol and fatty acid metabolism were enhanced in the soft variety. The measured variation in metabolite levels gave strong support to the precedent results. This study suggests that at fruit set, a composite scenario of active metabolic recycling of the cell wall, improved C: N balance and solute accumulation give place to a more efficient carbon and water resource management. During the ripe stage, an increased and efficient *in muro* and metabolic recycling of the cell wall, added to enhanced inositol and secondary metabolism may be responsible for a best turgor conservation in Emerald. These findings may yield clues for improvements in fertilization practices, as well as to assist the guided development of new varieties based on biochemical quality.

Keywords: blueberries, firmness, cell wall, metabolites, fatty acid, phenolic compounds, differential proteomic.

Introduction

Blueberries are appreciated by their pleasant appearance and flavour, as well as by their high content of bioactive molecules with a wide range of health benefits (Michalska and Łysiak, 2015).

The processes that govern ripening in this fruit are not entirely understood. They generate low levels of ethylene and are thus considered non-climacteric fruit (Frenkel, 1972; Lipe, 1978). One of the most appreciated quality trait is firmness, since a soft fruit would be frequently rejected by consumers. The causes of softening in fruits are diverse and involve events such as dehydration, cell wall dynamic, turgor and membranes damage, among others (Brummell, 2006a; Li et al., 2009; Paniagua et al., 2013; Vicente et al., 2007; Wang et al., 2018; Zoccatelli et al., 2013). In turn, these processes are deeply dependent on environmental conditions (i.e. soil composition, irrigation, climate, precipitation regime) and variety (Prodorutti et al., 2007; Sim et al., 2017; Zapata et al., 2010; Zhao, 2012). These are the major reasons for which literature about calcium fertilization, a frequent practice in blueberry cultivation, is not conclusive in terms of softening reduction (Angeletti et al., 2010; Basiouny and Woods, 1992; Berkheimer, E.J., Hanson, 2004; Stückrath et al., 2008).

Some highlights of blueberries production and commercialization in Argentina are relevant in defining the present research goals. For instance, the bulk of annual production is exported fresh and prime fruit have better prices. Thus, both the early production and the excellence in quality attributes are among the most relevant aspect to be considered by farmers and agronomists. Also, the facts that fruit is harvested stepwise due to non-homogeneous ripening, and that occasionally export is done by boat, cause that the time elapsed since the harvest and the arrival to final market location can exceed 30 days in some cases, seriously harming quality on destination. In sum, the above mentioned circumstances stress the need to establish the general quality determinants, and high firmness in particular at a molecular level as a main focus of research. In this sense, it is of interest for researchers involved in crop management assistance to gain knowledge about the molecular basis, i.e. the main compounds and biological processes that are connected with desirable traits. Previous work in which metabolomic and physiologic profiles were analysed in three blueberries varieties, gave some clues about a few chemical compounds and cell wall linked enzymes activities strongly correlated with fruit firmness (Montecchiarini et al., 2018). For this study, two of these varieties were selected according to their contrasting firmness: ‘Emerald’, highly productive, with large, good flavoured and very firm fruit and ‘O´Neal’, an early, very sweet, public cultivar with medium size and less firm fruit (http://www.fallcreeknursery.com/commercial-fruit-growers/varieties).

The main goal of this work is to use both the proteomic and metabolomic approaches to delve into how the differential molecular repertoire in two blueberries varieties at two phenological stages (set and full mature fruit), are linked to their contrasting quality. This information would contribute not only to design suitable crop management programs, but also it may provide agronomists with reliable methods for screening and selection of higher quality varieties.

Materials and Methods

Plant material, growth conditions and fruit sampling

Blueberries from 'Emerald' (U.S. Plant Patent 12165 P2) and 'O´Neal' cultivars were collected at local orchards in Concordia (Entre Ríos, Argentina, O´Neal lot Lat S: -31.398364, Long W: -58.107351; Emerald lot Lat S -31.32664, Long W -58.083086) during the morning, in 2016 season. Mature bushes used for field experiments were located in commercial fields, plants were grown on raised pine bark rows with a plant density of 3333 plants/ha. Standard agro-technical procedures were performed during the growing season. For frost protection, overhead sprinklers were used. The sampling dates in each cultivar were at 9 days after full bloom (DAFB) and 80 DAFB, corresponding to fruit set and ripe fruit (full blue fruit), respectively. Emerald blooms in July and harvest season spans from October to December, while O´Neal blooms in late July and is harvested from November to December. Data about precipitation levels, temperature fluctuation and time of harvesting are summarized in Figure 1. Thirty berries were collected from five different plants of each variety. After manual collection, exocarp and pulp (meso- and endocarp) were carefully separated for mature fruit. Samples were frozen at -80ºC until analysis. The reason to analyse the exocarp and the pulp separately is mainly to dissect the processes governing general quality and firmness in particular in each of these metabolically and anatomical different tissues. All the subsequent determinations were performed on the pulp of ripe berries, while entire fruit was used for fruit set analysis, due to the hindrance presented in the separation of tissues. At least three biological replicates were performed for all measures. Each replica was composed of a pool of three fruits.

Metabolite purification, derivatization and analysis

Samples were essentially treated as described by Perotti et al (2011). In brief, 300 mg of frozen tissue were powdered in a mortar with liquid nitrogen, 4.2 mL of cold methanol and 75 µg of ribitol (as internal standard) were added. Preparations were transferred to glass tubes and incubated at 70 °C for 15 min. After the addition of 1.5 mL of chloroform, samples were incubated 5 min at 37 °C. Finally, 3 mL of water were added and extracts were centrifuged at 2200×g and for 15 min. The polar phase (450 µL) was dried in a vacuum centrifuge (CentriVap, Labconco) until complete evaporation. Each pellet was resuspended in 30 µL of freshly prepared 20 mg/mL methoxyamine in pyridine, and tubes were incubated 90 min at 37ºC. Finally, 45 µL of derivatizing reactive, N-methyl-N-trimethylsylil-trifluoroacetamide (MSTFA) were added to each tube and incubated at 37 °C for 30 min. Chromatographic runs were performed by injecting 1 µL of derivatized sample (split: 1:100) in a 30 m long, 0.25 mm thick HP5ms UI GC/MS capillary column using an automatic system coupled to an Agilent simple quadrupole mass spectrometer (5977A). Data were analyzed using the OpenChrom software (http://www.openchrom.net) for peak area determination and the Automated Mass spectral Deconvolution and Identification System software (AMDIS) for compound identification. Chromatograms acquired were analyzed by comparing individual peak areas for each metabolite relative to that of ribitol, the internal standard. Data were revised using the Golm metabolome database from the Golm Metabolomic Institute (Germany) to confirm the identity of the compounds.

Fatty acid extraction, derivatization and analysis

Total esterified lipids were extracted from fruit as described before (Bligh and Dyer, 1959) with slight modifications. Approximately, 500 mg of tissue were powdered in a mortar with liquid nitrogen and then homogenized with 300 µl of distilled water, to obtain 0.8 ml of homogenate. Samples were transferred to glass tubes containing 6 mL of a methanol: chloroform (2:1) mixture. Each tube was shaken and incubated overnight at -20 °C. After centrifugation at room temperature for 5 min at 800 × g, supernatants were transferred to new glass tubes. One mL of chloroform and 1 mL of distilled water were added to each tube. Samples were centrifuged for 5 min at room temperature at 800 × g to facilitate phases separation. The lower phase was conserved and washed twice with 2 mL of 2 M KCl.

Tubes were centrifuged for 5 min at room temperature at 800 × g. Finally, after drying the chloroform phase under nitrogen atmosphere, pellets were resuspended with 0.5 mL of sodium methoxide diluted in anhydrous methanol in a 1:8 proportion. After incubation for 30 min at room temperature, 1 mL of 2 M HCl and 1 mL of hexane were added. Finally, the hexane (upper) phase was transferred to a new glass tube for chromatographic analysis. In all cases, 2 µl of derivatized samples were injected in a 30 m × 0.25 mm SUPELCOWAX-10 (Sigma) column coupled to a ThermoQuest mass spectrometer. The run was carried out isothermally for 30 min at 180 °C. Afterward, the temperature was increased at 12 °C/min to reach 240 °C. Data were collected and analyzed using the Lab Solution software (Shimadzu). In order to identify the different methylated fatty acids, the retention time and peaks obtained in the mass spectrum were compared with true standards (Sigma Aldrich) or with available data in NBS75K (National Bureau of Standards database, Perkin Elmer). After sample analysis and relative amount calculation of each fatty acid, the double bond index (DBI) was obtained. The DBI is a measure of lipid unsaturation and was calculated according to (Zhou et al., 2014) as follows: DBI double bond index = Σ (% unsaturated fatty acid × number of double bonds).

Alcohol insoluble residue (AIR) determination and ion content analysis

Cell wall polysaccharides as AIR were obtained according to the method described by Angeletti et al. (2010) with the following modifications: 1 g of tissue was ground, homogenized in 3 ml of ethanol and boiled for 45 min to inactivate enzymes. Calcium and other ions were measured in cell wall material as follows: 50 and 15 mg of AIR from set and ripe fruit respectively, were digested with 1 ml of concentrated HNO_3 at 100ºC for 5 hours. After sample dilution, ions were quantified by Inductively Coupled Plasma Mass Spectrometry (ICP-MS, Perkin Elmer Nexion 350X). Quantification was carried out using standards curves for each compound, results are informed as ng ion/mg AIR.

Total phenolic compounds determination

The determination of total phenolics content (TPC) was carried out using the Folin-Ciocalteu reagent as described by Velioglu et al. (1998). Powder obtained from 25 mg of frozen tissue was homogenized in 750 µl of buffer (80% methanol, 1% HCl) and it was left to extract for two hours. After centrifugation (25000 x g for 5 min), the supernatant was recovered and a re-extraction of the pellet was carried out. The reaction mixture was prepared with 150 µl of the combined supernatants obtained in the previous step and 150 µl of Folin-Ciocalteu reagent. After 3 min, 500 µl of sodium bicarbonate (20%) were added and the reaction was incubated for 120 min. Finally, absorbance at 730 nm was measured. Results were informed as gallic acid µg/mg of fresh weight. Three technical replicates were performed for each of the three biological replicates employed.

Total protein extraction and preparation for proteomic analysis

Protein extraction was performed according to Hurkman and Tanaka (1986) with some modifications. Two hundred mg of frozen tissue were ground with liquid nitrogen and homogenized with 2 ml of buffer (0.1 M Tris pH 8.8, 10 mM EDTA, 0.9 M sucrose, 1 mM PMSF, 0.4% (v/v) BME, 5% (p/v) PVPP). Four ml of phenol-Tris HCl (pH 8.8) were added, and the mixture was shaken and incubated at 4 °C for 30 min. After centrifugation at 5000 x g for 20 min, the phenolic phase was recovered and mixed with 5 volumes of 0.1 M ammonium acetate in methanol. After overnight protein precipitation at -20 °C, the pellet was washed three times with ammonium acetate, and once with 80% (v/v) cold acetone. Pellets were dried and solubilized in 8 M urea. Extractions were made in triplicate for each sample. Protein concentration was assayed with the bicinchoninic acid method (Thermo Scientific Pierce BCA Protein Assay Kit). A calibration curve was carried out using bovine serum albumin as standard.

Protein identification and analysis

Forty microgram of each protein extract were reduced for 45 min at 56 ºC using 10 mM DTT and alkylated for 40 min with 20 mM iodoacetamide at room temperature in the dark. Finally, proteins were precipitated by adding 100% (p/v) trichloroacetic acid to a final concentration of 20%, washed three times with cold acetone, and dried.

Protein preparations were sent to the Proteomics Core Facility of CEQUIBIEM at the University of Buenos Aires. Samples were resuspended in 50 mM $(NH_4)HCO_3$ at pH 8.0, digested overnight with sequencing-grade modified trypsin (Promega) and desalted with Zip-Tip C18 (Merck Millipore). Proteins were analyzed by nanoHPLC (EASY-nLC 1000, Thermo Scientific, Germany) coupled to a mass spectrometer with Orbitrap technology (Q-Exactive with High Collision Dissociation cell and Orbitrap analyzer, Thermo Scientific, Germany). Peptide Ionization was performed by electrospray. Data were analyzed with Proteome Discoverer 2.1 software (Thermo Scientific, Germany) for identification and area quantitation of each protein. Protein identification was performed using *Vitis vinifera* Uniprot protein collection as a reference (UP000009183; Feb 4, 2017; https://www.uniprot.org/proteomes/UP000009183).

Triplicate area values obtained were checked for missing values, and samples with no values or only one, were replaced with a minimal global one in order to allow comparisons within samples. The Perseus software v1.6.1.3 (Tyanova et al., 2016) was used to perform comparisons among samples area values and statistical tests. Upon analysis, proteins with a $\log_2$ (normalized area ratio) > |1| and p-value < 0.05 were considered as significantly accumulated within each sample comparison.

To characterize the proteins of interest, Uniprot identifiers were assigned to Phytozome IDs using *Vitis vinifera* Genoscope.12X database (https://phytozome.jgi.doe.gov/pz/portal.html#!info?alias=Org_Vviniferav), and used to search for pre-computed *Arabidopsis thaliana* assigned orthologs within this database.

Gene ontology enrichment analysis was carried out using Singular Enrichment Analysis (SEA) through AgriGO v2.0 (http://systemsbiology.cau.edu.cn/agriGOv2/index.php) and the plant GO-slim database as reference. In addition, ShinyGO v0.41 (Ge and Jung, 2018) was also used to perform gene ontology enrichment analysis as well as metabolic pathway networks enrichment through the Kyoto Encyclopedia of Genes and Genomes (KEGG) metabolic pathways collections for *Arabidopsis thaliana*. In all cases, enrichment studies were statistically tested by the Hypergeometric test performed with multiple testing correction using

Hochberg false discovery rate (FDR) correction and a significance level < 0.05 after correction.

Search strategy for cell wall metabolism-related proteins

In order to explore the nature of enzymes related with cell wall metabolism represented within the complete set of proteins recovered, a keyword search was performed in the *Vitis vinifera* Genoscope.12X proteome (Phytozome) using protein names. This search included alpha and beta galactosidases, endoglucanases, pectinmethylesterases (PME), polygalacturonases (PG), PME inhibitor proteins, PG inhibitor proteins, pectate liases, xyloglucan hydrolases, xylosidases and expansins. Afterwards, their amino acid sequences were retrieved and used to perform a basic local alignment (blastp; minimum e value: 10^{-10}) against the *Vitis vinifera* Uniprot proteome (UP000009183). In this manner,it was possible to assign some missing identities, and to finally search within our proteomics data for cell wall metabolism-related proteins using the identified proteins as bait.

Statistical procedures

Inferential statistics was carried out applying t-Student test with a significance level of 0.05, in order to identify data with statistically significant differences between varieties in each stage under study. The Sigma Stat Package was used for statistical analysis. Principal component analysis was performed with R package “FactoMineR” and “corrplot”.

Results

Metabolite and ion content in blueberries pulp at two maturation stages: fruit set and ripe

In order to detect the vast and diverse collection of molecules that characterize a cellular state, more than one method of analysis is usually required. In this sense, metabolomics is one of the most complex omics approaches, but is probably the best to portray the actual physiological status of the analyzed sample with high fidelity. Thus, by a combination of different techniques, the relative quantification of sugars, sugar alcohols, amino acids, organic acids, total phenolic compounds and fatty acids in the pulp of two blueberry varieties at two different maturation stages was carried out.

Ions quantification was performed in the AIR fraction, enriched in cell wall material. Ion levels were compared for each blueberry variety and are presented as the amount found in Emerald relative to that found in O´Neal (EM/ON ratio) at fruit set (Figure 2) and in ripe fruit (Figure 3). Numerical data and statistical analysis is informed in supplementary Table 1.

It is worth to mention that a number of metabolites, mainly free amino acids, were detected only in Emerald. These were proline (Pro), isoleucine (Ile), methionine (Met), ornithine (Orn), asparagine (Asn), xylose, threonic and galacturonic acid in fruit set; glutamine (Gln) and asparagine (Asn) in ripe stage (supplementary Table 1).

Organic acids. Citric acid content was significantly higher in O´Neal while malic acid predominated in Emerald at fruit set, as well as shikimic and caffeoylquinic acids (Fig. 2). In ripe fruit, all these compounds were prevailing in Emerald (Figure 3).

Sugars. No significant changes in the content of the main sugars were observed at fruit set (Figure 2). Sucrose content was higher in ripe O´Neal, without further variation for the additional major sugars, fructose and glucose (Figure 3).

Amino acids. Several amino acids, such as alanine (Ala), serine (Ser), valine (Val), threonine (Thr), Gln, aspartate (Asp), glutamate (Glu) and gamma aminobutyric acid (GABA) were more abundant in Emerald at fruit set. In ripe fruit, Ala, Ser, Asp and Glu predominated in Emerald, while Val content was higher in O´Neal (Figures 2 and 3).

Fatty acids. Major differences between fatty acids content were noticed at fruit set, when levels of 16:0, 22:0, 24:0, 16:1, 18:2 and 18:3 were higher in Emerald (Fig. 2). In ripe fruit, 18:1 level was higher in Emerald, while 18:0 and 17:0 predominated in O´Neal. DBI (double bond index) was calculated from these results and it was found to be higher for Emerald at both phenological stages (Figures 2 and 3).

Other compounds. The content of a cyclic polyalcohol, inositol, was higher in Emerald at both stages, while mannitol, also a sugar alcohol derived from hydrogenation of mannose, was only detected in ripe fruit and was more abundant in O´Neal. Total phenolic compounds (TPC) content was significantly higher in ripe fruit of Emerald (Figures 2 and 3).

Ion content in AIR. From the nine ions whose levels were quantified by ICP-MS in the AIR, two are considered as essential macronutrients (calcium and magnesium) and five as essential micronutrients (boron, iron, copper, manganese and zinc) (Benton Jones Jr., 2012). At fruit set, their levels were comparable between both varieties, with the exception made for aluminium, that was almost 3.2 times more abundant in O´Neal, and manganese which was 4.9 times higher in O´Neal. On the other hand, differences found in ripe fruit were significant only for manganese (3 times higher in O´Neal) and iron (2 times higher in Emerald) (Fig. 3). Calcium, frequently associated with cell wall strengthening, did not show significant differences between both varieties at any stage (Figures 2 and 3, supplementary Table 1).

With the aim of gaining insight into the metabolic association with differential traits in both varieties, data from metabolites that fluctuated significantly were subjected to Principal Component Analysis (PCA) (Figure 4). In this study, metabolites that were undetectable in O´Neal were excluded. Hence, at fruit set, PC1 (90.59%) was able to discriminate both varieties based on the following metabolites: manganese (contribution to individual PC of 4.54) which was predominant in O´Neal; while Ala (4.57), Val (4.71), Ser (4.72), Thr (4.67), malic acid (4.59), Asp (4.45), GABA (4.50), Glu (4.65), Gln (4.71), shikimic acid (4.68), and inositol (4.68) content was more abundant in Emerald. Meanwhile, in ripe fruit, PC1 (89.31%) allowed the separation between varieties, with Ala (4.95), Ser (5.07), Asp (4.88), Glu (4.87), citric acid (4.99), quinic acid (4.95), inositol (5.08) and TPC (5.00) content more abundant in Emerald, while Val (5.04), xylose (4.99), margaric acid (17:0) (4.81), and mannitol (4.72) predominated in O´Neal.

Therefore, at a first glance, the precedent results make it compelling to suggest that some metabolic pathways might be predominant in Emerald at fruit set, in contrast with

O´Neal. Proteomic analysis and subsequent data interconnection will shed light on the physiological significance of observed differences between both cultivars.

Functional characterization and identification of protein differentially expressed between varieties at each phenological stage

Proteomic analysis resulted in a total of 630 different proteins detected for the complete set of samples (data not shown). Comparisons between varieties at the same maturity stage were performed. Proteins whose relative abundance (EM/ON ratio) varied significantly were selected from Volcano plots generated by Perseus software, and their identities assigned based on *Vitis vinifera* proteome database and *A. thaliana* orthology (see materials and methods) (supplementary Table 2).

Functional analysis and enrichment of biological processes were determined with ShinyGO and AgriGO using *A. thaliana* orthologous gene names. The Kyoto Encyclopedia of Genes and Genomes (KEGG) database, linking genomic and functional information, allowed the systematic analysis of gene functions and metabolic pathways that overrepresented in each analysis (PlantGSEA).

Considering the same developmental stage, the first glaring difference was the magnitude of proteome change in each variety, as judged by the total number of proteins recovered as differentially abundant, being remarkably lower for O´Neal in both cases (Table 1).

During fruit set, 166 (159 non- redundant) proteins were more abundant in Emerald, while 21 (20 non- redundant) were in O´Neal (Table 1). Gene ontology analysis (AgriGO) for Emerald proteins indicated that biological processes terms were enriched in response to stimulus (71), mainly abiotic stimulus (38) and stress response (44)), and also metabolic (115) and cellular processes (128). Among metabolic processes the most represented were biosynthesis of primary metabolites (107), nitrogenated compounds (81) and catabolic processes (30). Cellular processes comprise mainly metabolic aspects such as generation of precursors and energy metabolites (19) and macromolecule metabolism (63). Other processes that appeared represented were gene expression (43), carbohydrate (21) and lipid (12) metabolic processes. Meanwhile, in O´Neal, processes such as response to stimulus (12; abiotic stimulus (5) and response to stress (8)) and post-embryonic development (5) were enriched. Notably, in Emerald 18 proteins clustered in the cell wall cellular component category, while this group was not found in O´Neal. Identity of these proteins is informed in Table 2.

In ripe fruits, 88 (84 non-redundant) proteins whose levels were significantly augmented in Emerald, correlated with metabolic processes (70), from them, cellular (61) and primary (58) metabolism categories were the most enriched. Response to stimulus term (49; abiotic stimulus (23), response to stress (27)) was enriched, as well as nitrogen compound biosynthesis (38), biosynthetic (42) and catabolic processes (16). Other categories were photosynthesis (6), carbohydrate (12) and lipid (11) metabolic processes. Once more, 10 proteins were categorized in Emerald as cell wall cellular component category (Table 2). In O´Neal 35 polypeptides were found, the majority of them were related with cellular processes (25) and metabolic processes (23), with photosynthesis (5) and generation of precursor metabolites and energy (5) as the most statistically significative terms.

A similar gene ontology analysis was carried out with the ShinyGO resource (see materials and methods), which enables the settlement of more detailed categories, useful to perform a further connection with related metabolomic data. Thus, at fruit set in Emerald, predominated the metabolic processes that included small molecules, carboxylic/organic acids and macromolecular complex subunit organization, as well as biosynthesis of organonitrogen compounds. These results were in coincidence with those obtained by AgriGO. Conversely, in O´Neal, response to inorganic substances, such as metal or cadmium and oxidation-reduction processes were the most dominant (supplementary Figure 1). In ripe fruit, Emerald displayed enrichment in carboxylic/organic acids, response to chemical and response to cadmium and metal ions. In ripe O´Neal, the prevalent processes were acyl-CoA and thioester metabolism, small molecules metabolism and response to metal ions (supplementary Figure 2).

Summary of metabolic pathways specific for each variety and stage of development

A further and complementary inspection of KEGG pathways performed with ShinyGO resource (supplementary Figure 3) indicated than in Emerald, at fruit set there was an increment in biosynthesis of secondary metabolites and amino acids (Val, Leu, ILe, Gly, Ser, Thr biosynthesis), general carbon metabolism (glycolysis/gluconeogenesis, TCA cycle, pyruvate, carbon fixation) and the proteasome and ribosome involving pathways. Other, less relevant, are the pentose phosphate pathway, carbon fixation, fatty acid, terpenoid, amino and nucleoside sugar metabolisms. In O´Neal, the most important were fatty acid, ß-alanine and carbon metabolisms. Others were secondary metabolites, glycolysis/gluconeogenesis, glyoxylate and dicarboxylate pathways.

Metabolic pathways more represented in ripe fruit were, in Emerald, biosynthesis of secondary metabolites, carbon metabolism (like pyruvate and carbon fixation), biosynthesis of amino acids (Arg, Phe, Tyr, Trp), glycolysis/gluconeogenesis (supplementary Figure 4). Other were Arg and Pro metabolism, Ala, Asp, Glu metabolism, ascorbate metabolism, fatty acid metabolism and terpenoid acid biosynthesis, amino and nucleoside sugar metabolic pathways. In O´Neal, the main routes were biosynthesis of secondary metabolites, TCA cycle, carbon fixation, pyruvate and fatty acid metabolism, fatty acid biosynthesis.

Enrichment in proteins related with carbohydrate and cell wall metabolism

Primary cell wall provides to each cell with mechanical integrity, structure and a contact interphase with other cells. In this complex network, three basic groups of components interact: cellulose, hemicelluloses and pectins. Pectins polysaccharides are rich in α-1,4-linked galacturonic acid (GalA) subunits and comprise rhamnogalacturonans (RG) I and II, homogalacturonans (HG), arabinans and galactans (Atmodjo et al., 2013). GalA residues in HG can support different degree of methylation, governed by pectin methyl esterase (PME) activity. Thus, highly unesterified HG can either be cross-linked with Ca^{2+} ions to form an egg-box structure that reinforces the wall, or be substrate for pectinolytic enzymes that stimulate wall loosening. Hemicelluloses include xyloglucans, xylans, glucomannans, arabinoxylans and callose. Xyloglucans have a backbone of ß-1,4- linked glucose residues, but also holds short side chains of xylose and galactose. This glycan cross-links with cellulose, strengthening the wall. While cellulose is synthesized directly in the plasma membrane, the other

constituents are formed in the Golgi apparatus by diverse glycosyl transferases and, after secretion, suffer modifications catalyzed by apoplastic enzymes (Oikawa et al., 2013). As a result, cell walls are not static entities. On the contrary, during development and cell expansion, a process of constant reorganization, hydrolysis, loosening and polymerization is carried out (Houston et al., 2016). Likewise, carbohydrate metabolism is crucial at all maturation stages, since it is involved in precursors and energy supply to the growing cell and in general homeostasis of proteins and lipids (Castellarin et al., 2016; Liu et al., 2007; Serrano et al., 2017). Diverse carbohydrates are in turn the raw material for cell wall components biosynthesis. Hence, to better characterize biochemical differences during each phenological stage in both varieties in terms of general fruit quality (and firmness in particular), two gene ontology categories were selected: carbohydrate metabolism (from biological processes GO) and cell wall (from cellular component GO). A complete description of these groups of proteins is given in Table 2.

From this selection, it is notable that, at fruit set, in Emerald several enzymes implicated in glycolysis, cytoskeletal organization, pentose and nucleotide sugars synthesis increase, in comparison with O´Neal. The α-subunit of pyrophosphate-dependent 6-phosphofructo-1-kinase (PFP alpha) was also higher. Notably, the enzyme involved in the committed step of inositol generation, myo-inositol 1- phosphate synthase (IPS) increased, and this is correlated with inositol enhanced levels (Figure 2). This metabolite, as well as its derivatives, play crucial roles in signal transduction, stress tolerance, phosphate storage, membrane development and the synthesis of ascorbic acid (Conde et al., 2015; Cui et al., 2013; Loewus and Murthy, 2000). UDP-glucose 6-dehydrogenase catalyses the production of UDP-glucuronic acid, providing nucleotide sugars for cell wall polymer synthesis. UDP-arabinopyranose mutase catalyses the reversible conversion of UDP-arabinopyranose to UDP-arabinofuranose and is involved in the biosynthesis of non-cellulosic polysaccharides components of cell wall. It is also notorious an increment in alpha-mannosidase, proteasome and ribosome related proteins, as well as in diverse proteins related with transport. In O´Neal, levels of enzymes that were found to be increased are connected with alcoholic fermentation, pectin demethylation and production of glycerol-3-phosphate, which may be involved in lipid biosynthesis (phospho and acyl lipids). A rise in the content of sucrose synthase (SuSy), two different isoforms for each variety, is probably linked to the predominant nature of blueberry fruit as sink organ, in which this activity is the responsible of sucrose utilization.

When these changes are analysed in Emerald ripe fruit, a few proteins displayed the same tendency than in the immature stage: pyruvate kinase, triose phosphate isomerase (TPI), transketolase, IPS, aldolase, UDP-arabinopyranose mutase and SuSy. An increment in the content of other enzymes, like xyloglucan endotransglucosylase/hydrolase (XET/H), glyoxalase, malate synthase and the ß-subunit of pyrophosphate-dependent 6-phosphofructo-1-kinase (PFP beta) was also observed. In O´Neal, the content of a chitinase was higher than in Emerald, as well as one glycosyl hydrolase, and enzymes related with glycolysis, gluconeogenesis and pyruvate destination.

Profile of proteins related with cell wall metabolism and water transport in the total set of original data

Since in the precedent analysis only proteins that significantly changed levels by a factor of two or more were considered, and a subgroup was related to cell wall, a further search of proteins related with cell wall metabolism was carried out within original data. In this analysis were included: α and ß galactosidases, endoglucanases, pectinmethylesterases (PME), polygalacturonases (PG), PME inhibitor proteins, PG inhibitor proteins, pectate liases, xyloglucan hydrolases, xylosidases and expansins (structural proteins in the cell wall) (Table 3). Aquaporins were added to this analysis as well, considering that water dynamics is deeply related to cell turgor, and hence to firmness, in plant cells (Wong et al., 2018).

From this group of proteins, only the content of three of them varied significantly in one cultivar with respect to the other. No sequence with similarity to PG could be identified. PME protein is more abundant at both stages in O´Neal than in Emerald, but more markedly at fruit set (125 times higher). Xyloglucan endotransglycosidase/ hydrolase (XET/H) level increases significantly in ripe Emerald fruit (85.50 times higher). In the case of aquaporins, two proteins from this family could be detected in blueberries, but only one of them showed a significant higher level in Emerald at fruit set (almost 36 times greater than in O´Neal).

Discussion

Blueberries of different species and varieties diverge in their quality traits, which in turn have direct impact in fruit shelf life (Lyrene, 2008; Ortiz et al., 2018; Zapata et al., 2010). Many of these structural attributes, related with cell walls and peripheral layers, are settled early in development (Brummell, 2006b; Konarska, 2015; Ng et al., 2015). Emerald is one of the varieties whose cultivated area has been increasing since it was first introduced in the NEA. Two main features influence its settlement as an appreciated cultivar, it is an early variety and it has high firmness (>1.8N, classification after (Moggia et al., 2017). However, not many studies have been conducted to ascertain the metabolic and physiologic basis of these traits. The main purpose of the precedent study, was to compare this cultivar with O´Neal, as a model of a soft fruit (firmness < 1.6N), at two phenological stages, with the hope to delineate the principal biochemical differences. It is opportune to bear in mind that some of the divergences noticed can be directly connected with the meteorological conditions prevailing when each stage of maturation is reached, which differ between varieties (see Figure 1). This can be the case for a higher DBI and 18:2 level in Emerald, contributing to balance membranes fluidity in a lower temperature context. However, some metabolites and metabolic routes can be envisaged as molecular signatures of each variety.

Solutes accumulation, nitrogen: carbon balance and cell wall recycling are enhanced in the firmer variety

Several of the biological processes that prevailed in Emerald at fruit set, are engaged in the biosynthesis of amino acids, organic acids and secondary metabolites that may account for an increased turgor pressure. Indeed, some works point to relations in solute accumulation between the apoplast and symplast of mesocarp cell of grapes as key regulators of turgor pressure during ripening (Wada et al., 2008; Zepeda et al., 2018). An increase in apoplastic solute concentration caused a loss of turgor toward the onset of ripening; the opposite would arise with cytosolic (symplastic) accumulation. GABA and proline, were related with osmotic adjustment in different studies (Bouché and Fromm, 2004; Szabados and Savouré, 2010; Verbruggen and Hermans, 2008), although they also

fulfil a range of additional functions. For instance, GABA may contribute to cytosolic pH regulation (Bouché and Fromm, 2004) or may act as a signal molecule in diverse biotic and abiotic stresses (Bao et al., 2014; Seifi et al., 2013). GABA is also a key metabolite connecting carbon and nitrogen metabolisms that involve cytosolic and mitochondrial reactions, contributing to C:N balance (Plaxton and Podestá, 2006). Among the further roles of proline in plants, it has been proposed to activate the shikimic acid pathway and thus increase secondary metabolites production (Silva et al., 2018). This particular imino acid is a constituent of the cell wall glycosylated family proteins, the so called PRPG or HRPGs, proteins rich in proline and hydroxyproline, with different degree of glycosylation (Kavi Kishor et al., 2015). Malate and citrate accumulate in the vacuole to sustain growth and also play roles in cytosolic pH balance. At the same time, a very active synthesis and turnover of proteins appear to take place, boosted by the increased content in several amino acids and proteins related with their synthesis as well as with proteasome pathway.

A key protein that also plays a role in water-plant status is aquaporin. It belongs to the major intrinsic protein (MIP) family, which include members that transport water, small molecules and elements such as urea, ammonia or boron (Maurel et al., 2015) across membranes. Two classes are broadly distributed in plants, plasma membrane intrinsic proteins (PIP) and tonoplast intrinsic proteins (TIP). In grapes, analysis of microarrays and correlation networks highlighted the strong co-expression relationships within the MIP family and genes involved in processes such as growth, cell division or cell redox homeostasis. Moreover, one of the strongest relationships was found between the MIP family and genes participating in cell wall modification and cell expansion (Schlosser et al., 2008; Wong et al., 2018). In strawberry, two types of aquaporins (PIP1 and 2) showed a differential expression pattern during ripening (Merlaen et al., 2018) and their expression levels were correlated with firmness (Alleva et al., 2010). In the present report, two proteins from the MIP family were detected in blueberries, being one of them almost 36 times more abundant in Emerald at fruit set. In this phenological stage, the main function of these water channels is probably related with the rapidly expanding fruit and diverse solutes accumulation, as was observed in young grape berries (Fouquet et al., 2008). In turn, cells may handle the transport across PIP by regulating their opening or closure in response to environmental conditions (Tournaire-Roux et al., 2003; Uehlein et al., 2008). Although in leaves they were implicated in CO_2 transport, this was not measured in fruit (Terashima and Ono, 2002).

In view that there were no significant differences regarding calcium content (Figure 1) or in AIR amount (data not shown), it is concluded that at this stage varieties did not differ substantially in cell wall synthesis nor in calcium bridges. Notwithstanding, it is possible that the structure of pectins and hemicelluloses are being intensively remodelled, as suggested by the increase in xylose and galacturonic acid levels (supplementary Table 1), as well as in enzymes that catalyze the biosynthesis of precursors of cell wall glycans (UDP-xyl synthase, UDP-6PGDH, UDP-arabinose mutase, UDP-glucose 4,6-dehydratase, for rhamnose synthesis), or cell wall hydrolysis (alpha-mannosidase) (supplementary Table 2). Other hydrolytic enzymes such as α and ß galactosidases did not change with respect to O´Neal, while PME protein levels were 125 times lower. PME activity, as mentioned before, generates free carboxylates in galacturonic residues of pectins, which may result in a more porous cell wall when combined with enhanced levels to hydrolytic enzymes; or may increase calcium coordination, strengthening the structure (Jolie et al., 2010). A hint about which processes are taking place can be provided by considering the dynamic nature of the wall. UDP-sugars are direct substrates

for *de novo* synthesis of all the glucans present in the cell wall. These carbohydrates constitute approximately the 45% of the total carbon fixed by year (Field et al., 1998), meaning that, far from accomplish only structural roles, cell wall carbohydrates are potential energy source and carbon sink that help to sustain growth and development. A growing body of evidences indicate that these roles are carried out by an intense cell wall recycling in plants (Barnes and Anderson, 2018). As it has been described above, not only the enzymes associated with synthesis, hydrolysis and remodelling of the wall, but also, the metabolites related, have been found increased in Emerald at fruit set. In addition, enzymes from glycolysis and gluconeogenesis (PGM, TPI, PK, enolase, FBPase, PFP alpha) or in pentose phosphate pathway, were increased, supporting a close relation between wall remodelling, precursors for recycling and associated energy supply.

Thus, it is tempting to hypothesize that a combination of an intense cell wall metabolic recycling, increased solute (and compatible solutes) and improved carbon to nitrogen balance, may contribute to a higher efficiency in water and carbon resources management in the firmer variety.

In ripe fruit, the firmer variety modulates in muro cell wall recycling, secondary metabolite synthesis and inositol metabolism

Plants are also able to cleave and reconnect polysaccharides *in muro,* i.e. inside the cell wall, and they perform this through a diverse sort of endo and exo-transglycosylases (Barnes and Anderson, 2018). This is another category of cell wall recycling mechanism, which does not require sugar internalization or its conversion to NDP-sugar substrate and glycosyltransferases activities, as metabolic recycling does. The action of transglycosylases allows to elongate and/or branch xyloglucans, tuning their links and interactions in this way. In ripe Emerald, one xyloglucan endotransglucosylase/hydrolase increased 85.5 times in comparison with O´Neal (Table 2). It belongs to a family of proteins that catalyse endotransglycosylation (XET) and/or xyloglucan endohydrolysis (XEH). These enzymes are involved in the modification of cell wall structure by cleaving and also re-joining xyloglucan molecules in primary plant cell walls. A few studies suggest that some members of this protein family have only the XET activity, being involved in cell wall remodelling (Langer et al., 2018; Nardi et al., 2014). The fact that xylose content was lower, supports the idea that the main activity displayed by this enzyme is as a transglucosylase instead of hydrolase. In addition, the increase in levels of other enzymes such as UDP-arabinose mutase, UDP- glucose 4,6- dehydratase, PFP beta subunit, mannose-1-phosphate guanylyltransferase, TPI and sugar transporters (supplementary Table 2), suggests that metabolic recycling is also taking place.

In a previous work done with three blueberry varieties, the activities of ß-galactosidase (ß-gal) and PME in green and ripe fruit (Montecchiarini et al., 2018) were mostly in agreement with enzymes levels reported here (Table 3). In fact, in the less firm variety (O´Neal) a combination of high PME and ß-gal activities in ripe fruit suggested that an association of a more soluble pectin in the presence of a high level of a hydrolytic enzyme could be in part the cause of a reduced firmness. Surprisingly, no sequence with similarity with polygalacturonase could be found within the proteomic data. This evidence, as well as the failure to measure PG activity at these stages (data not shown), could be pointing either to a very low activity or to some technical issues in the recovery of this enzyme for the in vitro colorimetric assay. However, other authors reported a failure to detect PG activity in grape berry or detected low transcript levels of related mRNA (Fasoli et al., 2016; Nunan et al., 2001). Moreover, a survey of transcripts of

enzymes related to cell wall metabolism in blueberries made it noticeable that polygalacturonases are poorly expressed and only at two intermediate phenological stages, not analysed here (Rowland et al., 2012). Thus, it is possible that other hydrolytic enzymes could be more relevant for blueberry softening than polygalacturonases.

Secondary metabolites encompass a vast group of specialized compounds synthesized from precursors arising out of primary metabolism. They are bioactive molecules with several health-promoting effects like polyphenols or flavonoids, very abundant in berries (Manganaris et al., 2014; Michalska and Łysiak, 2015). Phenolic compounds are related with diverse functions such as antioxidant capacity, herbivore defence or survival to different environmental conditions (Eichholz et al., 2011; Howard et al., 2003; Keutgen and Pawelzik, 2007). TPC content was higher in Emerald, and two of them, quinic and caffeoylquinic acids, have been identified in the metabolomic study. The accumulation of these compounds is genotype, variety and tissue dependent (Castrejón et al., 2008; Howard et al., 2003; Karppinen et al., 2016; Lee et al., 2014; Mikulic-Petkovsek et al., 2012), also influenced by maturation and field conditions (Teixeira et al., 2013). They are more abundant in exocarp and in the ripe stage and a role of these compounds in negatively regulating PME activity has been proved (Lewis et al., 2008), raising the possibility that they could be in part responsible for enhanced firmness in Emerald.

Myo- inositol, or simply inositol, biosynthesis is carried out by a two-step process in which IPS generates inositol-1-P from 6-phosphogluconate, which is later dephosphorylated by an inositol phosphatase to render inositol (Majumder et al., 1997). The first reaction is considered rate limiting for inositol accumulation. Relative level of this metabolite was higher in Emerald than in O´Neal at both stages, as it was IPS protein, but its role may be different in each stage. This sugar alcohol is related with several functions such as osmotic protection or scavenging of reactive oxygen radicals and in young fruit has been related with maintenance of turgor (Boldingh et al., 2000). In the same way, IPS expression is required for organ development in plants (Chen and Xiong, 2010) and it can be induced by a number of environmental stresses (Munnik and Vermeer, 2010; Valluru and Van den Ende, 2011; Wang et al., 2011). Decay in inositol phosphates pool in seedlings of tomato, mutant in one inositol phosphatase, increased the synthesis of secondary metabolites, although the unambiguous connection with inositol concentration was not established (Alimohammadi et al., 2012).

As mentioned before, changes in the contribution of solute concentration ratio between apoplast and symplast to turgor status in each development stage has been pointed for grape. In blueberry, conductivity measures of total pulp homogenates was significantly higher in ripe Emerald (data not shown) but the implication of this in cell turgor needs further research.

Mannitol is synthesized in source tissues and transported via phloem to sink tissues, as fruit and roots, where it can be stored and metabolized (Patel and Williamson, 2016). It is considered a compatible solute, as other polyols, sugars or amino acids, since its concentration may increase without altering the normal physiology of the cell. Its action is also thought to be due to its antioxidant capacity, as a ROS quencher (Jennings et al., 1998; Meena et al., 2015). Under low osmotic potential, mannitol may protect proteins and cellular structures by interacting with their hydration shell. Likewise, when water potential is low, under salt or drought stress, the damage caused by the increase in ROS concentration may be ameliorated by mannitol. An increase in the content of this metabolite in ripe O`Neal could be a response to a decrease in the water status of the

fruit. In fact, precipitation levels in its harvesting period were considerably lower than for Emerald (see Figure 1).

Conclusion

Metabolomic and proteomic studies described here provide useful and complementary information about factors that account for fruit quality in blueberries. Even though high firmness in fruit is the resultant of not fully understood connections between cell wall metabolism, water status and turgor pressure, it is possible to delineate some clues. Taking a soft variety (O´Neal) as a reference, it was possible to describe those compounds and metabolic processes that were most likely connected with general quality in the firmer variety (Emerald). During fruit set, Emerald´s higher levels of diverse metabolites, increased content of proteins related with cell wall metabolic recycling and water transport, point to a best handling of carbon, nitrogen and hydric resources at the onset of fruit development. Later on, in ripe fruit, increased content of secondary metabolites (phenolic compounds, quinic acid) and inositol, as well as *in muro* cell wall recycling, emerge as the key events possibly linked with firmness (Figure 5). Further research is needed to depict the site of solute accumulation and its relationship with cell turgor, for instance, employing specific probes and apoplast/symplast partition. In the same way, new fluorescent oligosaccharides compounds used for pulse-chase and confocal microscopy experiments could pave the way for the understanding of the contribution of cell wall recycling, degradation and sugar salvage to firmness maintenance. Future research will comprise the characterization of the proteome and metabolome of exocarp´s tissue, associated with physiologic and structural studies of other intermediate phenological stages.

Author contributions

KT, DV, FR and FEP conceived and designed the study. MM, EM, LM, performed the experiments and analysed the data. FR, FB, AG and DV carried out the crop treatments, samples collection and physiological studies. KT, FEP, MM and EM drafted the manuscript. All authors participated in the interpretation of data and the revision of the manuscript. All authors approved the submission and agreed to be accountable for all aspects of the work.

Conflict of interest statement

The authors declare that the research was conducted in the absence of any commercial or financial relationships that could be construed as a potential conflict of interest.

Funding

This work was supported by grants from the Agencia Nacional de Promoción Científica y Tecnológica to KEJT (PICT 2016-0091) and FEP (PICT 2015-1074). KEJT, FEP and EM are members of the investigator Career from the Consejo Nacional de Investigaciones Científicas y Técnicas (CONICET). MLM and LM are Doctoral Fellows of CONICET and AG is a Doctoral Fellow CONICET/INTA. FB, MFR and DV are members of the Instituto Nacional de Tecnología Agropecuaria (INTA).

Acknowledgments

The authors want to acknowledge the collaboration of Mónica Hourcade and Guillermo Marccuzzi for GC-MS runnings and to phD Ayelén Pagani for ICP-MS ion determinations.

References

Alimohammadi, M., De Silva, K., Ballu, C., Ali, N., and Khodakovskaya, M. V. (2012). Reduction of inositol (1,4,5)-trisphosphate affects the overall phosphoinositol pathway and leads to modifications in light signalling and secondary metabolism in tomato plants. *J. Exp. Bot.* 63, 825-3.

Alleva, K., Marquez, M., Villarreal, N., Mut, P., Bustamante, C., Bellati, J., et al. (2010). Cloning, functional characterization, and co-expression studies of a novel aquaporin (FaPIP2;1) of strawberry fruit. *J. Exp. Bot.* 61, 3935-45.

Angeletti, P., Castagnasso, H., Miceli, E., Terminiello, L., Concellón, A., Chaves, A., et al. (2010). Effect of preharvest calcium applications on postharvest quality, softening and cell wall degradation of two blueberry (Vaccinium corymbosum) varieties. *Postharv. Biol. Technol.* 58, 98–103.

Atmodjo, M. A., Hao, Z., and Mohnen, D. (2013). Evolving Views of Pectin Biosynthesis. *Annu. Rev. Plant Biol.* 64, 747-79.

Bao, H., Chen, X., Lv, S., Jiang, P., Feng, J., Fan, P., et al. (2014). Virus-induced gene silencing reveals control of reactive oxygen species accumulation and salt tolerance in tomato by γ-aminobutyric acid metabolic pathway. *Plant. Cell Environ.* 38, 600-13.

Barnes, W. J., and Anderson, C. T. (2018). Release, Recycle, Rebuild: Cell-Wall Remodeling, Autodegradation, and Sugar Salvage for New Wall Biosynthesis during Plant Development. *Mol. Plant*. 11, 31-46.

Basiouny, F. M., and Woods, F. (1992). Effect of chelated calcium on shelf-life and quality of blueberry fruits (Vaccinium ashei Reade). *Proc. Fla. State Hort. Soc* 105, 75-78.

Benton Jones Jr., J. (2012). *Plant Nutrition and Soil Fertility Manual*. Boca Raton, FL: CRC Press. Second Ed.

Berkheimer, E.J., Hanson, S. F. (2004). Effect of Soil Calcium Applications on Blueberry Yield and Quality. *Small Fruits Rev. Food Prod. Press. Haworth Press. Inc.* 3, 133-139.

Bligh, E. G., and Dyer, W. J. (1959). A rapid method of total lipid extraction and purification. *Can. J. Biochem. Physiol.* 37, 911-917.

Boldingh, H., Smith, G. S., and Klages, K. (2000). Seasonal concentrations of non-structural carbohydrates of five Actinidia species in fruit, leaf and fine root tissue. *Ann. Bot.* 85, 469-476.

Bouché, N., and Fromm, H. (2004). GABA in plants: just a metabolite? *Trends Plant Sci.* 9, 110-115.

Brummell, D. A. (2006a). Cell wall disassembly in ripening fruit. *Funct. Plant Biol.* 33, 103-119.

Brummell, D. A. (2006b). Primary cell wall metabolism during fruit ripening. *New Zeal. J. For. Sci.* 36, 99-111.

Castellarin, S. D., Gambetta, G. A., Wada, H., Krasnow, M. N., Cramer, G. R., Peterlunger, E., et al. (2016). Characterization of major ripening events during softening in grape: Turgor, sugar accumulation, abscisic acid metabolism, colour development, and their relationship with growth. *J. Exp. Bot.* 67, 709-22.

Castrejón, A. D. R., Eichholz, I., Rohn, S., Kroh, L. W., and Huyskens-Keil, S. (2008). Phenolic profile and antioxidant activity of highbush blueberry (Vaccinium corymbosum L.) during fruit maturation and ripening. *Food Chem.* 109, 564-572.

Chen, H., and Xiong, L. (2010). myo-Inositol-1-phosphate synthase is required for polar auxin transport and organ development. *J. Biol. Chem.* 285, 4238-47.

Conde, A., Regalado, A., Rodrigues, D., Costa, J. M., Blumwald, E., Chaves, M. M., et al. (2015). Polyols in grape berry: Transport and metabolic adjustments as a physiological strategy for water-deficit stress tolerance in grapevine. *J. Exp. Bot.* 66, 889-906.

Cui, M., Liang, D., and Ma, F. (2013). Molecular cloning and characterization of a cDNA encoding kiwifruit l-myo-inositol-1-phosphate synthase, a key gene of inositol formation. *Mol. Biol. Rep.* 40, 697-705.

Eichholz, I., Huyskens-Keil, S., Kroh, L. W., and Rohn, S. (2011). Phenolic compounds, pectin and antioxidant activity in blueberries (Vaccinium corymbosum L.) influenced by boron and mulch cover. *J. Appl. Bot. Food Qual.* 84, 26-32.

Fasoli, M., Dell'Anna, R., Dal Santo, S., Balestrini, R., Sanson, A., Pezzotti, M., et al. (2016). Pectins, Hemicelluloses and Celluloses Show Specific Dynamics in the Internal and External Surfaces of Grape Berry Skin during Ripening. *Plant Cell Physiol.* 57, 1332-1349.

Field, C. B., Behrenfeld, M. J., Randerson, J. T., and Falkowski, P. (1998). Primary production of the biosphere: Integrating terrestrial and oceanic components. *Science.* 281, 237- 240.

Fouquet, R., Léon, C., Ollat, N., and Barrieu, F. (2008). Identification of grapevine aquaporins and expression analysis in developing berries. *Plant Cell Rep.* 27,1541-50.

Frenkel, C. (1972). Involvement of Peroxidase and Indole-3-acetic Acid Oxidase Isozymes from Pear, Tomato, and Blueberry Fruit in Ripening. *Plant Physiol*. 49, 757–763.

Ge, S., and Jung, D. (2018). ShinyGO: a graphical enrichment tool for animals and plants. *bioRxiv*. doi:10.1101/315150.

Houston, K., Tucker, M. R., Chowdhury, J., Shirley, N., and Little, A. (2016). The Plant Cell Wall: A Complex and Dynamic Structure As Revealed by the Responses of Genes under Stress Conditions. *Front. Plant Sci.* doi:10.3389/fpls.2016.00984.

Howard, L. R., Clark, J. R., and Brownmiller, C. (2003). Antioxidant capacity and phenolic content in blueberries as affected by genotype and growing season. *J. Sci. Food Agric.* 83, 1238–1247.

Hurkman, W. J., and Tanaka, C. K. (1986). Solubilization of Plant Membrane Proteins for Analysis by Two-Dimensional Gel Electrophoresis. *Plant Physiol.* 81, 802-6.

Jennings, D. B., Ehrenshaft, M., Pharr, D. M., and Williamson, J. D. (1998). Roles for mannitol and mannitol dehydrogenase in active oxygen-mediated plant defense. *Proc. Natl. Acad. Sci.* 95, 15129-15133.

Jolie, R. P., Duvetter, T., Van Loey, A. M., and Hendrickx, M. E. (2010). Pectin methylesterase and its proteinaceous inhibitor: A review. *Carbohydr. Res.* 345, 2583-2595.

Karppinen, K., Zoratti, L., Nguyenquynh, N., Häggman, H., and Jaakola, L. (2016). On the Developmental and Environmental Regulation of Secondary Metabolism in Vaccinium spp. Berries. *Front. Plant Sci.* 7. doi:10.3389/fpls.2016.00655.

Kavi Kishor, P. B., Hima Kumari, P., Sunita, M. S. L., and Sreenivasulu, N. (2015). Role of proline in cell wall synthesis and plant development and its implications in plant ontogeny. *Front. Plant Sci.* 6, 544. doi:10.3389/fpls.2015.00544.

Keutgen, A. J., and Pawelzik, E. (2007). Modifications of strawberry fruit antioxidant pools and fruit quality under NaCl stress. in *J. Agric. Food Chem.*, 4066-4072.

Konarska, A. (2015). Morphological, anatomical and ultrastructural changes in Vaccinium corymbosum fruits during ontogeny. *Botany.* 93, 589-602.

Langer, S. E., Oviedo, N. C., Marina, M., Burgos, J. L., Martínez, G. A., Civello, P. M., et al. (2018). Effects of heat treatment on enzyme activity and expression of key genes controlling cell wall remodeling in strawberry fruit. *Plant Physiol. Biochem.* 130, 334-344.

Lee, S., Jung, E. S., Do, S. G., Jung, G. Y., Song, G., Song, J. M., et al. (2014). Correlation between species-specific metabolite profiles and bioactivities of blueberries (Vaccinium spp.). *J. Agric. Food Chem.* 62, 2126–2133.

Lewis, K. C., Selzer, T., Shahar, C., Udi, Y., Tworowski, D., and Sagi, I. (2008). Inhibition of pectin methyl esterase activity by green tea catechins. *Phytochemistry* 69, 2586–2592.

Li, C., Shen, W., Lu, W., Jiang, Y., Xie, J., and Chen, J. (2009). 1-MCP delayed softening and affected expression of XET and EXP genes in harvested cherimoya fruit. *Postharv. Biol. Technol.* 52, 254–259.

Lipe, J. A. (1978). Ethylene in fruits of blackberry and rabbiteye blueberry. *J. Am. Soc. Hortic. Sci.*103, 76-77.

Liu, Y.-B., Lu, S.-M., Zhang, J.-F., Liu, S., and Lu, Y.-T. (2007). A xyloglucan endotransglucosylase/hydrolase involves in growth of primary root and alters the deposition of cellulose in Arabidopsis. *Planta* 226, 1547- 1560.

Loewus, F. A., and Murthy, P. P. N. (2000). myo-Inositol metabolism in plants. *Plant Sci.* 150, 1-19.

Lyrene, P. M. (2008). "Emerald" southern highbush blueberry. *HortScience* 43, 1606-1607.

Majumder, A. L., Johnson, M. D., and Henry, S. A. (1997). 1L-myo-Inositol-1-phosphate synthase. *Biochim. Biophys. Acta - Lipids Lipid Metab.* 1348, 245-256.

Manganaris, G. A., Goulas, V., Vicente, A. R., and Terry, L. A. (2014). Berry antioxidants: Small fruits providing large benefits. *J. Sci. Food Agric.* 94, 825- 833.

Maurel, C., Boursiac, Y., Luu, D.-T., Santoni, V., Shahzad, Z., and Verdoucq, L. (2015). Aquaporins in Plants. *Physiol. Rev.* 95, 1321-1358.

Meena, M., Prasad, V., Zehra, A., Gupta, V. K., and Upadhyay, R. S. (2015). Mannitol metabolism during pathogenic fungal-host interactions under stressed conditions. *Front. Microbiol.* doi:10.3389/fmicb.2015.01019.

Merlaen, B., De Keyser, E., and Van Labeke, M. C. (2018). Identification and substrate prediction of new Fragaria x ananassa aquaporins and expression in different tissues and during strawberry fruit development. *Hortic. Res.* doi:10.1038/s41438-018-0019-0.

Michalska, A., and Łysiak, G. (2015). Bioactive compounds of blueberries: Post-harvest factors influencing the nutritional value of products. *Int. J. Mol. Sci.* 16, 18642-18663.

Mikulic-Petkovsek, M., Schmitzer, V., Slatnar, A., Stampar, F., and Veberic, R. (2012). Composition of Sugars, Organic Acids, and Total Phenolics in 25 Wild or Cultivated Berry Species. *J. Food Sci.* 77, 1064-1070.

Moggia, C., Graell, J., Lara, I., González, G., and Lobos, G. A. (2017). Firmness at Harvest Impacts Postharvest Fruit Softening and Internal Browning Development in Mechanically Damaged and Non-damaged Highbush Blueberries (Vaccinium corymbosum L.). *Front. Plant Sci.* 8, 535. doi:10.3389/fpls.2017.00535.

Montecchiarini, M., Bello, F., Rivadeneira, M., Vazquez, D., Podestá, F., and Tripodi, K. (2018). Metabolic and physiologic profile during the fruit ripening of three blueberries highbush (Vaccinium corymbosum) cultivars. *J. Berry Res.* 8, 177-192.

Munnik, T., and Vermeer, J. E. M. (2010). Osmotic stress-induced phosphoinositide and inositol phosphate signalling in plants. *Plant, Cell Environ.* 33, 655-669.

Nardi, C. F., Villarreal, N. M., Opazo, M. C., Martínez, G. A., Moya-León, M. A., and Civello, P. M. (2014). Expression of FaXTH1 and FaXTH2 genes in strawberry fruit. Cloning of promoter regions and effect of plant growth regulators. *Sci. Hortic. (Amsterdam).*165, 111-122.

Ng, J. K. T., Schröder, R., Brummell, D. A., Sutherland, P. W., Hallett, I. C., Smith, B. G., et al. (2015). Lower cell wall pectin solubilisation and galactose loss during early fruit development in apple (Malus x domestica) cultivar "Scifresh" are associated with slower softening rate. *J. Plant Physiol.* 176, 129-137.

Nunan, K. J., Davies, C., Robinson, S. P., and Fincher, G. B. (2001). Expression patterns of cell wall-modifying enzymes during grape berry development. *Planta*. 214, 257-264.

Oikawa, A., Lund, C., and Sakuragi, S. (2013). Golgi-localized enzyme complGolgi-localized enzyme complexes for plant cell wall biosynthesis. *Trends Plant Sci.* 18, 49-58.

Ortiz, C., Franceschinis, F., Gergoff Grozeff, G., Chan, H., Labavitch, J., Crisosto, C., et al. (2018). Pre-treatment with 1-methylcyclopropene alleviates methyl bromideinduced

internal breakdown, softening and wall degradation in blueberry. *Postharv. Biol. Technol.* 146, 90- 98.

Paniagua, A. C., East, A. R., Hindmarsh, J. P., and Heyes, J. A. (2013). Moisture loss is the major cause of firmness change during postharvest storage of blueberry. *Postharv. Biol. Technol.* 79, 13- 19.

Patel, T. K., and Williamson, J. D. (2016). Mannitol in Plants, Fungi, and Plant–Fungal Interactions. *Trends Plant Sci.* 6, 486-497.

Perotti, V. E., Del Vecchio, H. A., Sansevich, A., Meier, G., Bello, F., Cocco, M., et al. (2011). Proteomic, metabalomic, and biochemical analysis of heat treated Valencia oranges during storage. *Postharv. Biol. Technol.* 62, 97- 114.

Plaxton, W. C., and Podestá, F. E. (2006). The Functional Organization and Control of Plant Respiration. *CRC. Crit. Rev. Plant Sci.* 25, 159- 198.

Prodorutti, D., Pertot, I., Giongo, L., and Gessler, C. (2007). Highbush Blueberry : Cultivation , Protection , Breeding and Biotechnology. *Eur. J. Plant Sci. Biotechnol.* 1, 44- 56.

Rowland, L. J., Bell, D. J., Alkharouf, N., Bassil, N. V., Drummond, F. A., Beers, L., et al. (2012). Generating Genomic Tools for Blueberry Improvement. *Int. J. Fruit Sci.* 12, 276- 287.

Schlosser, J., Olsson, N., Weis, M., Reid, K., Peng, F., Lund, S., et al. (2008). Cellular expansion and gene expression in the developing grape (Vitis vinifera L.). *Protoplasma*. 232, 255-265.

Seifi, H. S., Curvers, K., De Vleesschauwer, D., Delaere, I., Aziz, A., and Höfte, M. (2013). Concurrent overactivation of the cytosolic glutamine synthetase and the GABA shunt in the ABA-deficient sitiens mutant of tomato leads to resistance against Botrytis cinerea. *New Phytol.* 199, 490- 504.

Serrano, A., Espinoza, C., Armijo, G., Inostroza-Blancheteau, C., Poblete, E., Meyer-Regueiro, C., et al. (2017). Omics Approaches for Understanding Grapevine Berry Development: Regulatory Networks Associated with Endogenous Processes and Environmental Responses. *Front. Plant Sci.* doi:10.3389/fpls.2017.01486.

Silva, F. L. B., Vieira, L. G. E., Ribas, A. F., Moro, A. L., Neris, D. M., and Pacheco, A. C. (2018). Proline accumulation induces the production of total phenolics in transgenic tobacco plants under water deficit without increasing the G6PDH activity. *Theor. Exp. Plant Physiol.* 30, 251- 260.

Sim, I., Suh, D. H., Singh, D., Do, S. G., Moon, K. H., Lee, J. H., et al. (2017). Unraveling Metabolic Variation for Blueberry and Chokeberry Cultivars Harvested from Different Geo-Climatic Regions in Korea. *J. Agric. Food Chem.* doi:10.1021/acs.jafc.7b04065.

Stückrath, R., Quevedo, R., De La Fuente, L., Hernández, A., and Sepúlveda, V. (2008). Effect of foliar application of calcium on the quality of blueberry fruits. *J. Plant Nutr.* 31, 1299- 1312.

Szabados, L., and Savouré, A. (2010). Proline: a multifunctional amino acid. *Trends*

Plant Sci. 15, 89- 97.

Teixeira, A., Eiras-Dias, J., Castellarin, S. D., and Gerós, H. (2013). Berry phenolics of grapevine under challenging environments. *Int. J. Mol. Sci.* 14, 18711-18739.

Terashima, I., and Ono, K. (2002). Effects of HgCl(2) on CO(2) dependence of leaf photosynthesis: evidence indicating involvement of aquaporins in CO(2) diffusion across the plasma membrane. *Plant Cell Physiol.* 43, 70-78.

Tournaire-Roux, C., Sutka, M., Javot, H., Gout, E., Gerbeau, P., Luu, D. T., et al. (2003). Cytosolic pH regulates root water transport during anoxic stress through gating of aquaporins. *Nature*. 425, 393-397.

Tyanova, S., Temu, T., and Cox, J. (2016). The MaxQuant computational platform for mass spectrometry-based shotgun proteomics. *Nat. Protoc.* 11, 2301-2319.

Uehlein, N., Otto, B., Hanson, D. T., Fischer, M., McDowell, N., and Kaldenhoff, R. (2008). Function of Nicotiana tabacum Aquaporins as Chloroplast Gas Pores Challenges the Concept of Membrane CO2 Permeability. *PlantCellOnline*. doi:10.1105/tpc.107.054023.

Valluru, R., and Van den Ende, W. (2011). Myo-inositol and beyond - Emerging networks under stress. *Plant Sci.* 181, 387-400.

Velioglu, Y. S., Mazza, G., Gao, L., and Oomah, B. D. (1998). Antioxidant Activity and Total Phenolics in Selected Fruits, Vegetables, and Grain Products. *J. Agric. Food Chem.* 46, 4113–4117.

Verbruggen, N., and Hermans, C. (2008). Proline accumulation in plants: A review. *Amino Acids*. 35, 753- 759.

Vicente, A. R., Saladié, M., Rose, J. K. C., and Labavitch, J. M. (2007). The linkage between cell wall metabolism and fruit softening: Looking to the future. *J. Sci. Food Agric.* 87, 1435- 1448.

Wada, H., Shackel, K. A., and Matthews, M. A. (2008). Fruit ripening in Vitis vinifera: Apoplastic solute accumulation accounts for pre-veraison turgor loss in berries. *Planta*. 227, 1351- 1361.

Wang, D., Yeats, T. H., Uluisik, S., Rose, J. K. C., and Seymour, G. B. (2018). Fruit Softening: Revisiting the Role of Pectin. *Trends Plant Sci.* 23, 302-310.

Wang, Y., Huang, J., Gou, C. B., Dai, X., Chen, F., and Wei, W. (2011). Cloning and characterization of a differentially expressed cDNA encoding myo-inositol-1-phosphate synthase involved in response to abiotic stress in Jatropha curcas. *Plant Cell. Tissue Organ Cult.* 106, 269-277.

Wong, D. C. J., Zhang, L., Merlin, I., Castellarin, S. D., and Gambetta, G. A. (2018). Structure and transcriptional regulation of the major intrinsic protein gene family in grapevine. *BMC Genomics* 19, 248. doi:10.1186/s12864-018-4638-5.

Zapata, L. M., Malleret, A. D., Quinteros, C. F., Lesa, C. E., Vuarant, C. O., Rivadeneira, M. F., Gerard, J.A. (2010). Estudio sobre cambios de la firmeza de bayas de arándanos durante su maduración. *Ciencia, Docencia y Tecnol.* 21, 159-171.

Zepeda, B., Olmedo, P., Ejsmentewicz, T., Sepúlveda, P., Balic, I., Balladares, C., et al. (2018). Cell wall and metabolite composition of berries of Vitis vinifera (L.) cv. Thompson Seedless with different firmness. *Food Chem.* 268, 492-497.

Zhao, Y. (2012). Auxin biosynthesis: A simple two-step pathway converts tryptophan to indole-3-Acetic acid in plants. in *Mole. Plant*, 334–338.

Zhou, Y., Pan, X., Qu, H., and Underhill, S. J. R. (2014). Low temperature alters plasma membrane lipid composition and ATPase activity of pineapple fruit during blackheart development. *J. Bioenerg. Biomembr.* 46, 59-69.

Zoccatelli, G., Zenoni, S., Savoi, S., Dal Santo, S., Tononi, P., Zandonà, V., et al. (2013). Skin pectin metabolism during the postharvest dehydration of berries from three distinct grapevine cultivars. *Aust. J. Grape Wine Res.* 19, 171–179.

Figure captions

Figure 1. Precipitation levels and temperature fluctuation during the period of harvesting for each variety at each phenological stage.

Figure 2. EM/ON ratio of metabolite, ion, TPC content and DBI at fruit set. X axis has a logarithmic scale. Purple bars indicate that there is a statistically significant difference between varieties (α=0.05, supplementary Table 1). Graph was constructed using R package "ggplot2".

Figure 3. EM/ON ratio of metabolite, ion, TPC content and DBI in ripe fruit. X axis has a logarithmic scale. Purple bars indicate that there is a statistically significant difference between varieties (α=0.05, supplementary Table 1). Graph was constructed using R package "ggplot2".

Figure 4. PCA of data at fruit set (A) and at ripe stage (B). In each case, only data that showed statistically significant difference between varieties were used. Three independent replicates were analyzed for each variety. The variance explained by each component (%) is given within parentheses. Plots at the right of each PCA indicate the correlation between each metabolite and both of the principal components (PC1 and 2). Positive correlations are displayed in white, while negative correlations in black. The size of the circle is proportional to the correlation coefficient.

Figure 5. Differential processes in Emerald. Molecular and metabolic processes that are enhanced in the firmer variety at both phenological stages.

Tables

Table 1. Functional classification of proteins differentially expressed in Emerald compared to O´Neal. Proteins from supplementary Table 2 were analyzed with AgriGO. Categories for GO: Biological Processes and GO: Cellular Component (cell wall) increased in each cultivar and phenological stage (FDR < 0.05), are summarized.

Table 2. Detail of proteins classified in the carbohydrate metabolism (GO: Biological Process) and cell wall (GO: Cellular Component) that are differentially expressed in each phenological stage and variety. The identity (*A. thaliana*

orthologous) and a description of these proteins were recovered after proteomic analysis as described in materials and methods.

Table 3. Identity and pattern of variation of proteins related to cell wall metabolism in Emerald versus O´Neal at both maturity stages. The search of these cell wall related proteins was carried out following the strategy outlined in materials and methods. Numbers indicate ratio between protein levels in Emerald and O´Neal. nc: no change, ns: non significative change.

Supplementary Figure 1. Biological processes enrichment at fruit set in Emerald and O´Neal varieties. Analysis was conducted with ShinyGO resource using data orthologous identities from *A. thaliana* (in Suppl. Table 2). Numbers indicate the FDR.

Supplementary Figure 2. Biological processes enrichment in ripe fruit in Emerald and O´Neal varieties. Analysis was conducted with ShinyGO resource using data orthologous identities from *A. thaliana* (in Suppl. Table 2). Numbers indicate the FDR.

Supplementary Figure 3. KEGG pathways more represented in Emerald and O´Neal varieties at fruit set. Analysis was conducted with ShinyGO KEGG resource using data orthologous identities from *A. thaliana* (in Suppl. Table 2). Numbers indicate the FDR.

Supplementary Figure 4. KEGG pathways more represented in Emerald and O´Neal varieties in ripe fruit. Analysis was conducted with ShinyGO KEGG resource using data orthologous identities from *A. thaliana* (in Suppl. Table 2).

Supplementary Table 1. **Metabolites, TPC, ions and fatty acids content at fruit set and ripe stage.** Levels of metabolites, TPC, ions and fatty acids in ON and EM, at different maturity stages (fruit set and ripe stage). Values (± SD) represent the mean of 3 independent determinations. T-test was performed and p-values are submitted.

Supplementary Table 2. Description of proteins differentially expressed in Emerald and O`Neal fruit at two phonological stages. Perseus software v1.6.1.3 (Tyanova et al, 2016) was used to perform comparisons among normalized area values of proteomic study for each sample. Upon analysis, and statistical tests, proteins with a log2 (normalized area ratio) > |1| and p-value < 0.05 were selected.

Table 1

Stage: FRUIT SET				**Stage: FRUIT SET**			
Variety: Emerald				**Variety: O´Neal**			
GO_acc Biological Process	**Term**	**Number of hits (total: 159)**	**FDR**	**GO_acc Biological Process**	**Term**	**Number of hits (total: 20)**	**FDR**
GO:0044237	cellular metabolic process	115	5.2e-20	GO:0050896	response to stimulus	12	0.0041
GO:0009987	cellular process	128	1.7e-18	GO:0006950	response to stress	8	0.013
GO:0008152	metabolic process	119	1.9e-15	GO:0009791	post-embryonic development	5	0.02
GO:0044238	primary metabolic process	107	1.9e-15	GO:0009628	response to abiotic stimulus	5	0.043
GO:0006807	nitrogen compound metabolic process	81	1.9e-14	GO:0009987	cellular process	14	0.065
GO:0009058	biosynthetic process	77	2.7e-12	GO:0008152	metabolic process	13	0.089
GO:0006091	generation of precursor metabolites and energy	19	4.8e-12	GO:0007275	multicellular organism development	5	0.09

GO:0044249	cellular biosynthetic process	72	2.8e-11	GO:0032501	multicellular organismal process	5	0.1
GO:0009628	response to abiotic stimulus	38	2.5e-10	GO:0032502	developmental process	5	0.1
GO:0050896	response to stimulus	71	1.4e-09	GO:0048856	anatomical structure development	5	0.1
GO:0009056	catabolic process	30	2.8e-09	GO:0044237	cellular metabolic process	10	0.16
GO:0006412	translation	27	4.8e-07	GO:0009058	biosynthetic process	6	0.33
GO:0006950	response to stress	44	8.5e-07	GO:0044249	cellular biosynthetic process	5	0.46
GO:0044267	cellular protein metabolic process	46	1.5e-06	GO:0006807	nitrogen compound metabolic process	5	0.49
GO:0019538	protein metabolic process	49	2.00E-06				
GO:0005975	carbohydrate metabolic process	21	8.2e-06				
GO:0016043	cellular component organization	32	2.2e-05				
GO:0006139	nucleobase-containing compound metabolic process	42	3.1e-04				
GO:0044260	cellular macromolecule metabolic process	63	4.5e-04				
GO:0043170	macromolecule metabolic process	66	0.001				
GO:0015979	photosynthesis	7	0.0019				
GO:0010467	gene expression	43	0.002				
GO:0034645	cellular macromolecule biosynthetic process	40	0.0037				
GO:0009059	macromolecule biosynthetic process	40	0.0045				
GO:0007275	multicellular organism development	27	0.0096				
GO:0048856	anatomical structure development	29	0.012				
GO:0040007	growth	10	0.012				
GO:0032501	multicellular organismal process	28	0.012				
GO:0032502	developmental process	29	0.015				
GO:0009719	response to endogenous stimulus	18	0.018				
GO:0006629	lipid metabolic process	12	0.021				
GO:0009790	embryo development	8	0.03				
GO:0006810	transport	21	0.049				
Cellular component GO:0005618	cell wall	18	2.2e-07				

Table 2

Stage: FRUIT SET					
BIOLOGICAL PROCESS: Carbohydrate metabolic processes	***A. thaliana* orthologous**	**Description**	**BIOLOGICAL PROCESS: Carbohydrate metabolic processes**	***A. thaliana* orthologous**	**Description**
Increased in Emerald	AT3G02360	6-phosphogluconate dehydrogenase family protein	*Increased in O´Neal*	AT4G02280	Sucrose synthase 3
	AT3G52990	Pyruvate kinase family protein		AT1G77120	Alcohol dehydrogenase related
	AT3G06580	Mevalonate/galactokinase family protein		AT4G34200	D-3-phosphoglycerate dehydrogenase, chloroplastic
	AT3G22960	Plastidic pyruvate kinase beta subunit 1		AT1G12900	Glyceraldehyde-3-phosphate dehydrogenase, A subunit, chloroplastic
	AT5G15490	UDP-glucose 6-dehydrogenase family protein		AT3G14310	Pectin methylesterase 3
	AT3G55440	Triosephosphate isomerase			
	AT2G28760	UDP-xylose synthase 6			
	AT3G22200	PLP-dependent transferases superfamily protein			
	AT2G22240	Myo-inositol-1-phosphate synthase 2			
	AT5G50850	Transketolase family protein			
	AT5G58330	Lactate/malate dehydrogenase family protein			
	AT5G03650	Starch branching enzyme 2.2			
	AT2G36530	Enolase			
	AT3G02230	UDP-arabinopyranose mutase			
	AT5G13980	Alpha-mannosidase			
	AT3G59480	PfkB-like carbohydrate kinase family protein			
	AT2G01140	Fructose bisphosphate aldolase, chloroplastic related			
	AT4G24620	Phosphoglucose isomerase 1			
	AT3G43190	Sucrose synthase 4			
	AT3G25860	Dihydrolipoamide acetyltransferase component of pyruvate DH complex			

	AT1G59900	Pyruvate dehydrogenase complex E1 alpha subunit		
	AT1G20950	Pyrophosphate-dependent 6-phosphofructose-1-kinase (alfa subunit)		

Table 3

UNIPROT ID	**Description**	**FRUIT SET**	**RIPE**
		EM/ON	*EM/ON*
A3FA66	Aquaporin PIP14	35.97	nc
A3FA63	Aquaporin PIP11	nc	nc
F6HJ88	Xyloglucan endotransglucosylase/hydrolase	nc	85.50
F6HEX2	α-D-xyloside xylohydrolase /α-xylosidase	nc	1.43 ns
D7SQ37	Xylose isomerase	0.37 ns	0.80 ns
F6HGZ1	Pectin methyl esterase (PME)	0.008	0.45
F6I1A6	β-galactosidase	nc	0.87 ns
D7TXW8	α-galactosidase	nc	nc
D7SN69	UDP-apiose/xylose synthase	nc	nc

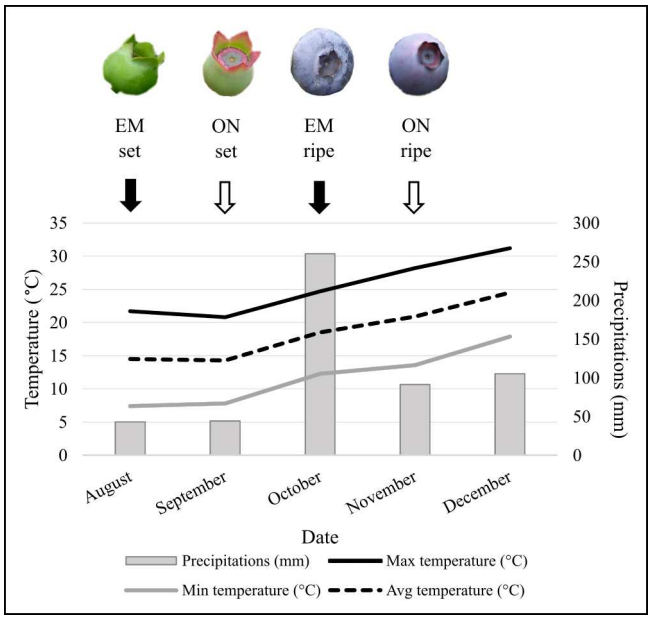

Figure 1

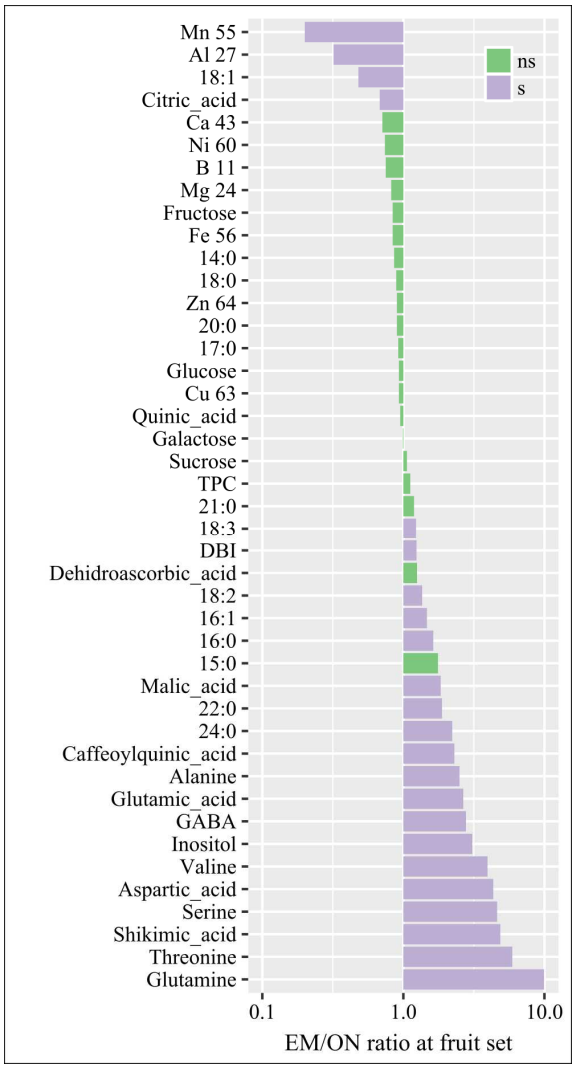

Figure 2

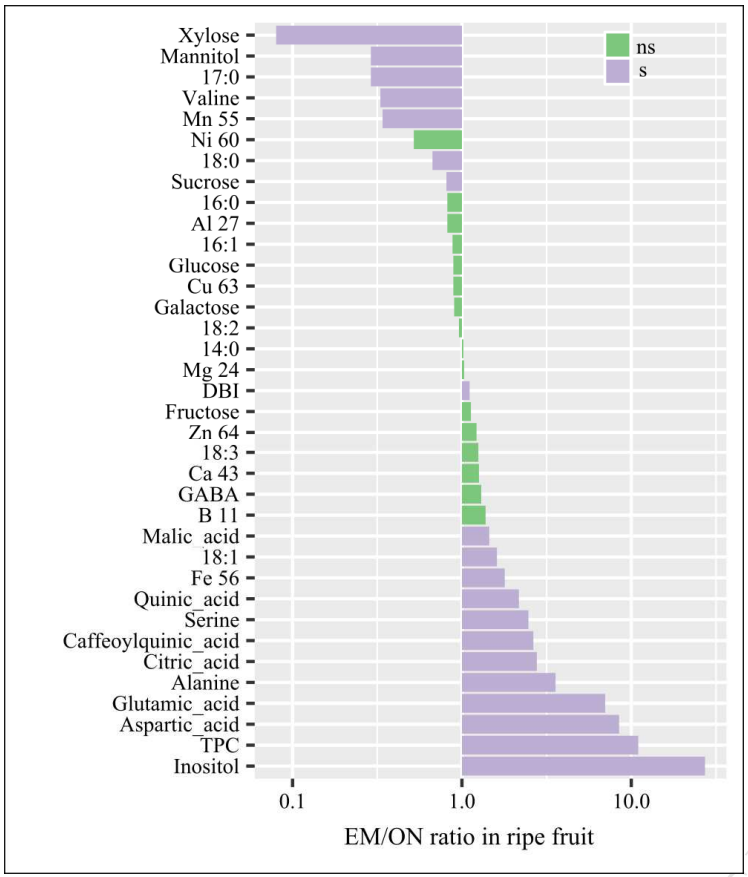

Figure 3

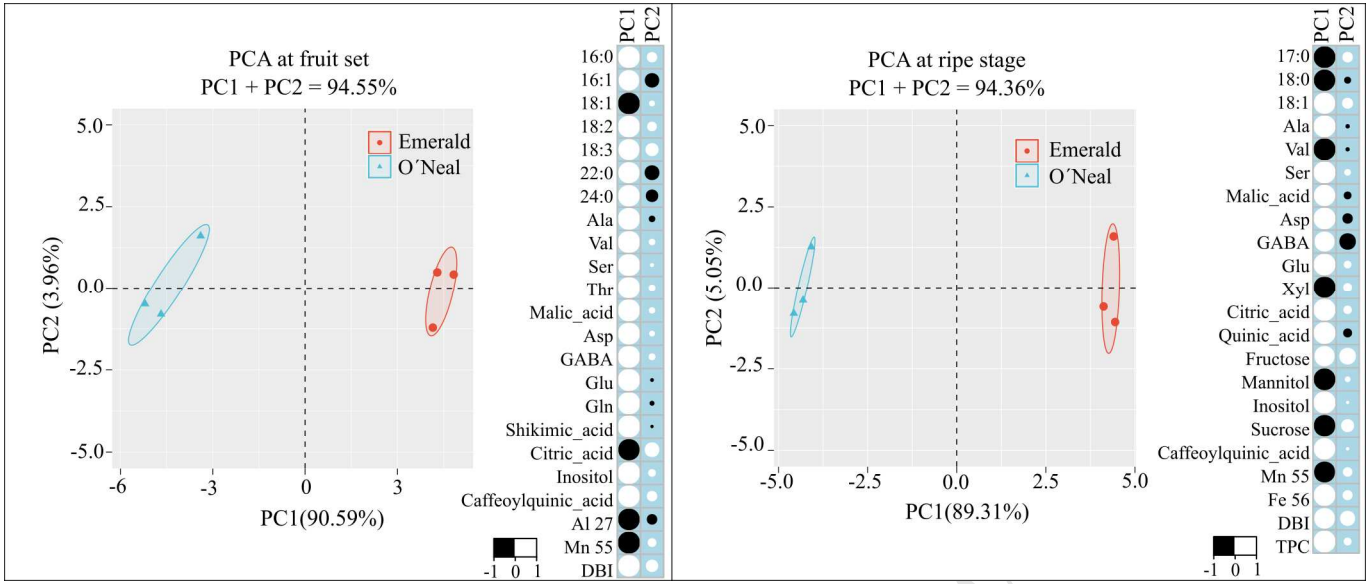

Figure 4

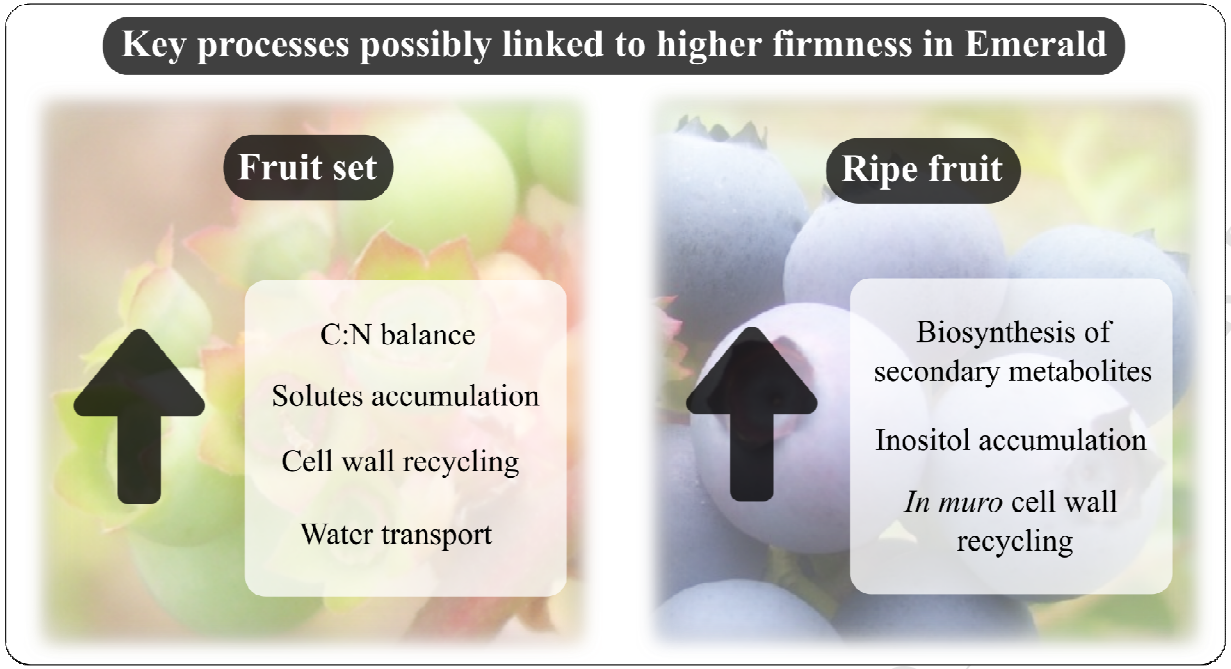

Figure 5

Supplementary Figure 1. Biological processes enrichment at fruit set in Emerald and O´Neal varieties. Analysis was conducted with ShinyGO resource using data orthologous identities from *A. thaliana* (in supplementary Table 2). Numbers indicate the FDR.

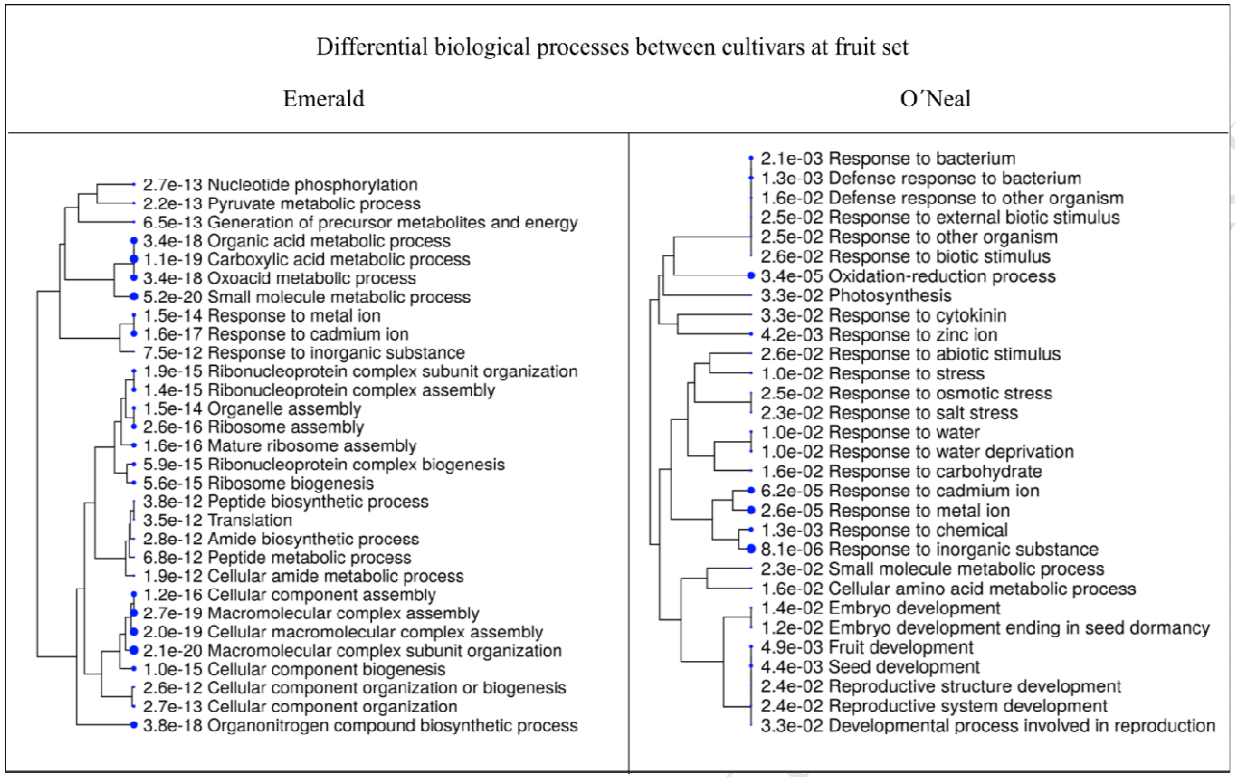

Supplementary Figure 2. Biological processes enrichment in ripe fruit in Emerald and O´Neal varieties. Analysis was conducted with ShinyGO resource using data orthologous identities from *A. thaliana* (in Suppl. Table 2). Numbers indicate the FDR.

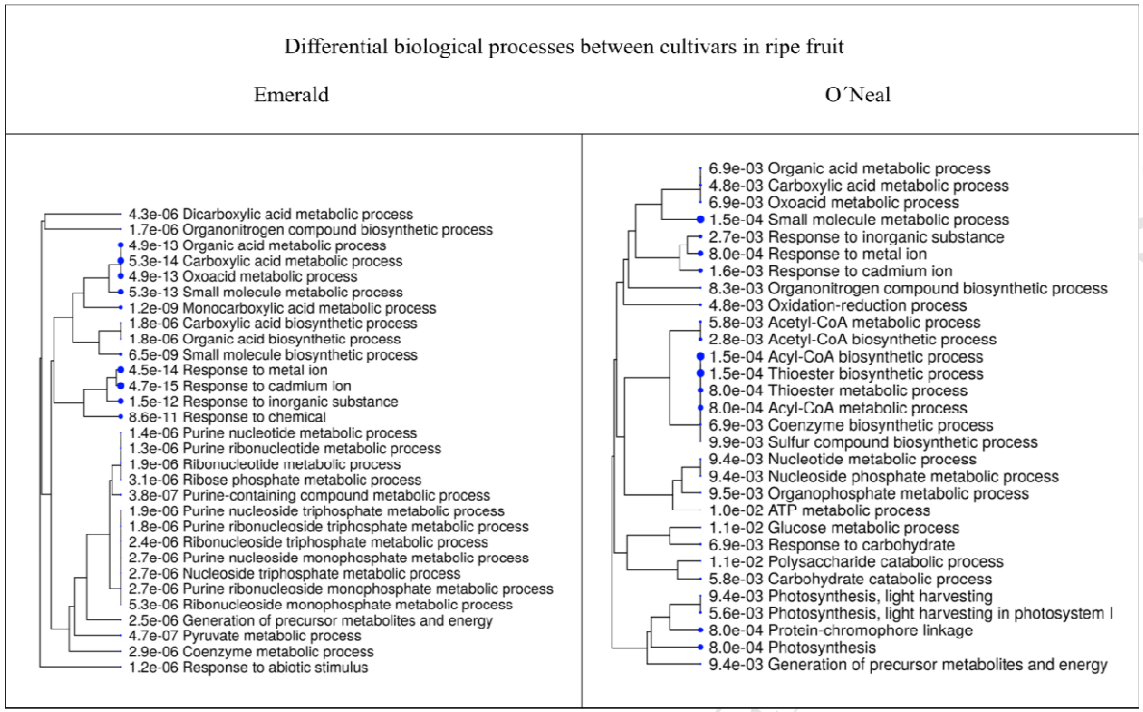

Supplementary Figure 3. KEGG pathways more represented in Emerald and O´Neal varieties at fruit set. Analysis was conducted with ShinyGO KEGG resource using data orthologous identities from *A. thaliana* (in Suppl. Table 2). Numbers indicate the FDR.

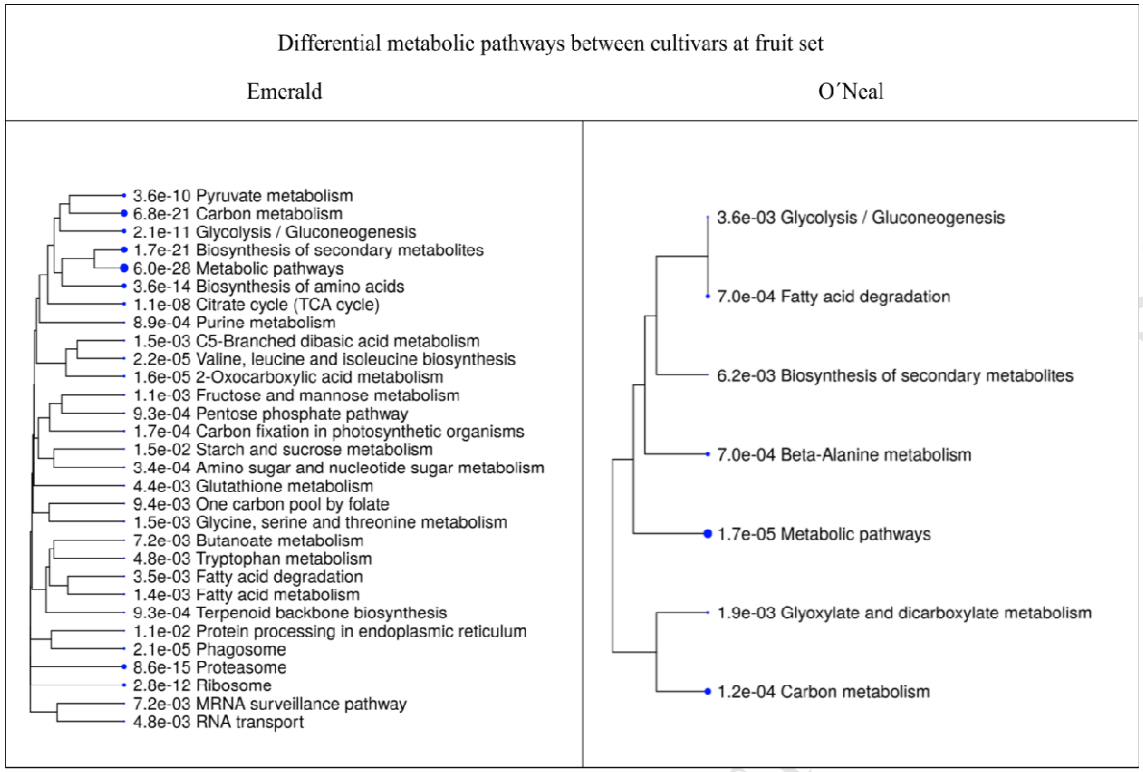

Supplementary Figure 4. KEGG pathways more represented in Emerald and O´Neal varieties in ripe fruit. Analysis was conducted with ShinyGO KEGG resource using data orthologous identities from *A. thaliana* (in Suppl. Table 2).

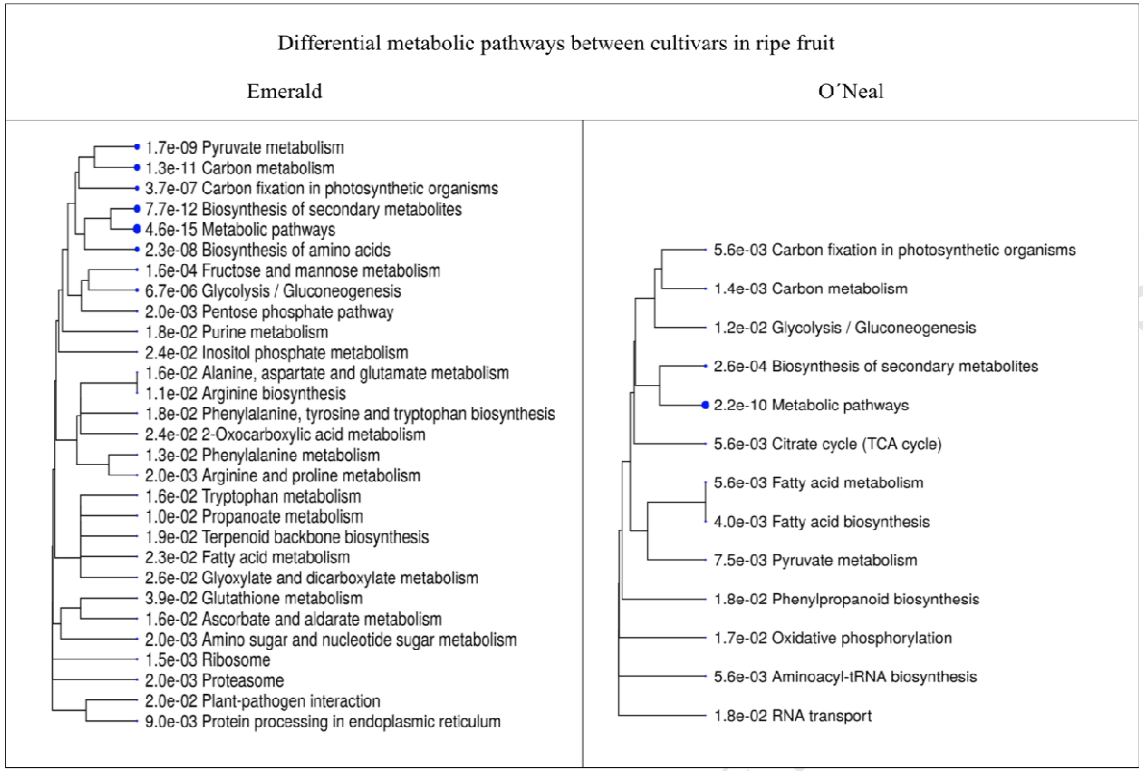

Supplementary Table 1. Metabolites, TPC, ions and fatty acids content at fruit set and ripe stage. Content determination of metabolites, TPC, ions and fatty acids in ON and EM, at different maturity stages (fruit set and ripe stage). Values (± SD) represent the mean of 3 independent determinations. T-test was performed and p-values are submitted.

Stage: FRUIT SET						
	Emerald	**SD**	**O´Neal**	**SD**	**EM/ON ratio**	**P-value**
Metabolites (relative area/gFW)						
Alanine	5.17	0.27	2.06	0.45	2.5	0.0005
Valine	1.73	0.11	0.44	0.16	4.0	0.0028
Proline	1.11	0.10	ND	/	/	/
Isoleucine	2.44	0.14	ND	/	/	/
Serine	3.13	0.19	0.68	0.19	4.6	0.0001
Threonine	0.44	0.07	0.07	0.03	5.9	0.0011
Methionine	0.42	0.05	ND	/	/	/
Malic_acid	9.58	0.95	5.20	0.25	1.8	0.0015
Aspartic_acid	3.12	0.42	0.72	0.38	4.3	0.0018
GABA	1.91	0.29	0.69	0.11	2.8	0.0023
Threonic_acid	1.43	0.10	ND	/	/	/
Ornithine	7.26	0.66	ND	/	/	/
Glutamic_acid	2.64	0.20	0.99	0.07	2.7	0.0002
Asparagine	1.49	0.04	ND	/	/	/
Xylose	0.11	0.05	ND	/	/	/
Glutamine	7.45	0.65	0.75	0.06	9.9	0.0008
Shikimic_acid	48.19	3.90	9.90	0.80	4.9	0.0004
Citric_acid	224.03	15.10	331.42	30.21	0.7	0.0053
Dehidroascorbic_acid	1.50	0.19	1.20	0.35	1.3	0.2589
Quinic_acid	632.15	125.74	668.73	62.31	0.9	0.6751
Fructose	106.88	7.70	126.91	12.45	0.8	0.0768

Galactose	159.47	9.91	160.98	13.95	1.0	0.8858
Glucose	27.46	2.23	29.49	2.36	0.9	0.3402
Galacturonic_acid	1.13	0.07	ND	/	/	/
Inositol	66.68	6.91	21.61	4.70	3.1	0.0007
Sucrose	20.48	3.96	19.40	3.69	1.1	0.7469
Caffeoylquinic_acid	222.92	41.49	96.97	19.80	2.3	0.0090
Fatty acids (percentage area/gFW)						
14:0	1.25	0.11	1.45	0.43	0.9	0.4861
15:0	0.38	0.09	0.21	0.09	1.8	0.0885
16:0	35.41	1.60	21.74	5.13	1.6	0.0116
16:1	1.63	0.26	1.11	0.04	1.5	0.0272
17:0	1.00	0.05	1.09	0.28	0.9	0.6141
18:0	6.05	0.62	6.78	1.84	0.9	0.5523
18:1	6.99	0.43	14.43	2.78	0.5	0.0445
18:2	74.58	0.50	54.82	5.99	1.4	0.0295
18:3	84.83	1.71	68.91	9.23	1.2	0.0425
20:0	3.24	0.51	3.61	0.75	0.9	0.5148
21:0	0.38	0.03	0.32	0.01	1.2	0.0795
22:0	1.71	0.23	0.91	0.16	1.9	0.0077
24:0	1.56	0.24	0.70	0.12	2.2	0.0052
Ions (ng ion/mg AIR)						
Ca 43	2268.98	595.79	3191.34	1001.23	0.7	0.2422
Mn 55	353.20	40.49	1738.51	295.94	0.2	0.0151
Cu 63	3.51	0.29	3.78	1.10	0.9	0.7044
Zn 64	30.11	9.76	33.56	9.99	0.9	0.6908
Al 27	43.78	19.25	138.67	39.57	0.3	0.0202
Fe 56	66.68	16.22	78.95	15.20	0.8	0.3933

B 11	9.46	1.77	12.70	1.31	0.7	0.1184
Ni 60	1.45	0.52	1.94	0.28	0.7	0.2189
Mg 24	1330.57	212.07	1622.59	619.31	0.8	0.4828
TPC (µg galic acid/mg FW)	95.31	5.86	85.17	15.11	1.1	0.4630
DBI	412.26	4.03	331.92	36.03	1.2	0.0180
Stage: RIPE FRUIT						
	Emerald	**SD**	**O´Neal**	**SD**	**EM/ON ratio**	**P-value**
Metabolites (relative area/gFW)						
Alanine	8.41	0.99	2.35	0.08	3.6	0.0089
Valine	1.28	0.08	3.93	0.17	0.3	<0.0001
Serine	3.87	0.13	1.57	0.11	2.5	<0.0001
Malic_acid	1.10	0.06	0.76	0.09	1.5	0.0054
Aspartic_acid	2.30	0.31	0.27	0.19	8.5	0.0006
GABA	2.01	0.28	1.55	0.09	1.3	0.0531
Glutamic_acid	3.39	0.57	0.48	0.07	7.0	0.0129
Asparagine	0.41	0.13	ND	/	/	/
Xylose	0.05	0.04	0.57	0.04	0.1	0.0001
Glutamine	1.80	1.06	ND	/	/	/
Citric_acid	146.06	4.66	52.64	11.58	2.8	0.0002
Quinic_acid	47.46	2.85	21.85	1.58	2.2	0.0002
Fructose	1150.81	61.28	1019.40	57.03	1.1	0.053
Galactose	1360.11	366.36	1511.58	653.11	0.9	0.7438
Glucose	229.25	59.05	258.87	108.98	0.9	0.7002
Mannitol	0.34	0.10	1.17	0.19	0.3	0.0024
Inositol	24.09	0.44	0.88	0.65	27.2	0.001
Sucrose	8.48	0.69	10.44	0.16	0.8	0.0089
Caffeoylquinic_acid	0.94	0.15	0.36	0.11	2.6	0.0053

Fatty acids (percentage area/gFW)						
14:0	1.24	0.98	1.21	0.06	1.0	0.9678
16:0	29.56	12.01	36.25	3.67	0.8	0.4088
16:1	0.80	0.41	0.91	0.03	0.9	0.6883
17:0	0.25	0.06	0.89	0.12	0.3	0.0068
18:0	4.87	0.22	7.24	0.81	0.7	0.0081
18:1	39.58	5.88	24.52	2.84	1.6	0.0162
18:2	102.47	11.17	107.24	4.62	1.0	0.5323
18:3	64.17	7.97	51.40	3.59	1.2	0.0647
Ions (ng /mg AIR)						
Ca 43	1785.19	739.05	1421.35	357.28	1.3	0.4855
Mn 55	96.85	32.90	281.98	77.79	0.3	0.0192
Cu 63	10.68	3.43	12.05	2.51	0.9	0.6055
Zn 64	20.48	7.35	16.84	3.74	1.2	0.4873
Zn 66	20.65	7.74	16.95	4.04	1.2	0.5033
Al 27	52.60	4.57	64.47	5.74	0.8	0.0941
Fe 54	900.43	213.09	567.14	131.73	1.6	0.0825
Fe 57	853.56	192.23	564.18	134.69	1.5	0.0996
Fe 56	956.26	42.95	533.85	116.39	1.8	0.0181
B 11	17.16	7.73	12.44	4.70	1.4	0.4171
Ni 60	8.26	1.83	15.87	2.85	0.5	0.1581
Mg 24	606.73	85.58	587.77	99.07	1.0	0.8406
TPC (µg galic acid/mg FW)	1.55	0.22	0.14	0.06	11.0	0.0126
DBI	437.84	11.52	394.11	20.83	1.1	0.0335

Supplementary Table 2. Description of proteins differentially expressed in Emerald and O`Neal fruit at two phenological stages. Perseus software v1.6.1.3 (Tyanova et al, 2016) was used to perform comparisons among normalized area values of proteomic study for each sample. Upon analysis, and statistical tests, proteins with a log2 (normalized area ratio) > |1| and p-value < 0.05 were selected.

Stage	Uniprot ID	Description	EM/ON	Log2	Phytozome DB *V.vinifera*	Orthologous gen *A. thaliana*
Fruit set Higher in EM	D7TI76	Tubulin alpha-5	1060.64	10.05	GSVIVT01033415001	AT5G19780.1
	D7SVZ9	myo-inositol-1-phosphate synthase 2	819.76	9.68	GSVIVT01022158001	AT2G22240.1
	F6HKH3	Enolase	708.69	9.47	GSVIVT01033770001	AT2G36530.1
	E0CVD7	Nascent polypeptide-associated complex subunit alpha-like protein 2	626.01	9.29	GSVIVT01038657001	AT3G49470.1
	D7T9I6	Proteasome subunit alpha	511.90	9.00	GSVIVT01012066001	AT1G79210.3
	F6HGH4	6-phosphogluconate dehydrogenase family protein	490.86	8.94	GSVIVT01010170001	AT3G02360.2
	A5BE97	Histone H2A 12	458.50	8.84	GSVIVT01025019001	AT5G02560.1
	A5AUZ0	40S Ribosomal protein S8e family protein	408.52	8.67	GSVIVT01031566001	AT5G59240.1
	A5B605	Eukaryotic elongation factor 5A-1	386.05	8.59	GSVIVT01007954001	AT1G13950.1
	A5B8T3	pfkB-like carbohydrate kinase family protein	360.01	8.49	GSVIVT01010790001	AT3G59480.1
	A5AJ83	Ribosomal protein S10p	352.30	8.46	GSVIVT01018553001	AT3G45030.1
	F6I019	Ribosomal protein L13 family protein	351.74	8.46	GSVIVT01028661001	AT3G24830.1
	D7TRL3	40S Ribosomal protein S6e	351.08	8.46	GSVIVT01003418001	AT5G10360.1
	F6HLL3	60S Ribosomal protein L6 family protein	335.16	8.39	GSVIVT01033532001	AT1G74050.1
	D7U016	Nucleosome assembly protein 1;2	334.60	8.39	GSVIVT01016870001	AT2G19480.3
	F6GUN2	Mitochondrial substrate carrier family protein	330.49	8.37	GSVIVT01025463001	AT5G19760.1
	A5AGN5	Ketol-acid reductoisomerase	326.77	8.35	GSVIVT01020689001	AT3G58610.3
	D7UA21	Calreticulin 1b	325.28	8.35	GSVIVT01031229001	AT1G09210.1
	A5ASW8	Chlorophyll a-b binding protein/light harvesting complex photosystem II subunit 6	324.45	8.34	GSVIVT01029789001	AT1G15820.1
	F6HUC8	Tubulin beta chain/beta-6 tubulin	307.12	8.26	GSVIVT01019758001	AT5G12250.1

	F6H5S6	FTSH protease 6	301.96	8.24	GSVIVT01011397001	AT5G15250.1
	A5BM68	Translationally controlled tumor protein	298.45	8.22	GSVIVT01017723001	AT3G16640.1
	F6GTX4	40S Ribosomal protein S12/S23 family protein	283.33	8.15	GSVIVT01016341001	AT5G02960.1
	F6I4L5	Heat shock protein 70 (Hsp 70) family protein	278.32	8.12	GSVIVT01031125001	AT5G42020.2
	F6HXY7	60S Ribosomal protein L6 family	273.95	8.10	GSVIVT01016795001	AT4G10450.1
	F6I1P0	Pyruvate dehydrogenase E1 component subunit beta /Transketolase family protein	268.48	8.07	GSVIVT01000944001	AT5G50850.1
	A5ALB2	20S proteasome subunit	268.38	8.07	GSVIVT01016731001	AT2G05840.1
	D7SH25	60S Ribosomal protein	260.55	8.03	GSVIVT01008585001	AT3G62870.1
	F6I0W2	Isocitrate dehydrogenase 1	259.99	8.02	GSVIVT01023949001	AT4G35260.1
	F6GVV0	60S Ribosomal protein	259.43	8.02	GSVIVT01036540001	AT3G62870.1
	D7U2H8	Calreticulin 1a	258.93	8.02	GSVIVT01028114001	AT1G56340.2
	D7TF52	60S ribosomal protein L13	252.48	7.98	GSVIVT01027212001	AT3G49010.1
	A5BX54	Isocitrate dehydrogenase [NADP]. cytosolic	241.23	7.91	GSVIVT01035240001	AT1G65930.1
	F6HMP3	Isopropyl malate isomerase large subunit 1	240.26	7.91	GSVIVT01029978001	AT4G13430.1
	D7SLS3	60S Ribosomal protein L23	238.64	7.90	GSVIVT01018183001	AT4G16720.1
	F6GTY8	Translation elongation factor EF1A	237.25	7.89	GSVIVT01015660001	AT5G10630.2
	F6GUQ0	RAN binding protein 1	229.51	7.84	GSVIVT01024705001	AT5G58590.1
	F6HFS7	60S Ribosomal L27e protein family	228.98	7.84	GSVIVT01012080001	AT4G15000.1
	F6H0X2	Phospho-2-dehydro-3-deoxyheptonate aldolase	225.85	7.82	GSVIVT01009070001	AT1G22410.1
	F6HFL6	Fructose-bisphosphate aldolase	223.46	7.80	GSVIVT01011810001	AT2G01140.1
	D7TZA8	Plastid transcriptionally active 17	221.12	7.79	GSVIVT01017471001	AT1G80480.1
	F6HI46	Acyl-CoA N-acyltransferase with RING/FYVE/PHD-type zinc finger protein	220.69	7.79	GSVIVT01001168001	AT1G05380.2
	F6GZY7	Granulin repeat cysteine protease family protein	211.14	7.72	GSVIVT01009440001	AT5G43060.1
	F6HBK3	Pyridoxal phosphate (PLP)-dependent transferases superfamily protein	207.88	7.70	GSVIVT01036981001	AT4G33680.1
	D7SHT5	T-complex protein 1 subunit gamma /cpn60 chaperonin family protein	207.68	7.70	GSVIVT01007770001	AT5G26360.1
	D7SKL7	60S ribosomal protein L23AB	197.66	7.63	GSVIVT01025041001	AT3G55280.2
	D7SKH2	Actin 1	197.40	7.62	GSVIVT01024980001	AT2G37620.1
	A5BEM6	Glutamate-1-semialdehyde 2.1-aminomutase 2	196.65	7.62	GSVIVT01008589001	AT3G48730.1

	F6HBZ6	D-3-phosphoglycerate dehydrogenase	189.18	7.56	GSVIVT01009428001	AT4G34200.1
	F6GZY2	D-3-phosphoglycerate dehydrogenase	187.82	7.55	GSVIVT01009428001	AT4G34200
	F6H8F3	Phosphoserine aminotransferase	187.36	7.55	GSVIVT01006497001	AT2G17630.1
	A5B5N0	Poly(A) binding protein 2	184.76	7.53	GSVIVT01009455001	AT4G34110.1
	A5C3G7	Gamma carbonic anhydrase 1	183.99	7.52	GSVIVT01009735001	AT1G19580.1
	F6HGZ9	Sucrose synthase 4	181.15	7.50	GSVIVT01015018001	AT3G43190.1
	D7U0H2	RAB GTPase homolog G3D	174.36	7.45	GSVIVT01017061001	AT1G52280.1
	A5BEF3	Regulatory particle AAA-ATPase 2A	173.48	7.44	GSVIVT01028520001	AT4G29040.1
	D0VBC7	3-phosphoshikimate 1-carboxyvinyltransferase	170.80	7.42	GSVIVT01027673001	AT2G45300.1
	A5AX75	General regulatory factor 11	170.41	7.41	GSVIVT01009037001	AT1G34760.1
	A5ALT5	DNAJ homologue 2	169.39	7.40	GSVIVT01036049001	AT5G22060.1
	F6HZ60	60S ribosomal protein L18	167.86	7.39	GSVIVT01028036001	AT3G05590.1
	F6I120	Amidase family protein	167.71	7.39	GSVIVT01024064001	AT4G34880.1
	F6GTE2	Reversibly glycosylated polypeptide 1	165.57	7.37	GSVIVT01008552001	AT3G02230.1
	D7TQM9	Isocitrate dehydrogenase V	164.04	7.36	GSVIVT01025704001	AT5G03290.1
	D7TJ87	Probable small nuclear ribonucleoprotein G	163.43	7.35	GSVIVT01033867001	AT2G23930.1
	F6HTM6	Pyridoxal phosphate (PLP)-dependent transferases superfamily protein	158.43	7.31	GSVIVT01015824001	AT3G22200.1
	D7T9L8	Clathrin adaptor complexes medium subunit family protein	155.89	7.28	GSVIVT01012108001	AT5G05010.1
	D7U9U7	Regulatory particle triple-A ATPase 5A	152.07	7.25	GSVIVT01031137001	AT3G05530.1
	F6H6E9	Fibrillarin 2	151.86	7.25	GSVIVT01028887001	AT4G25630.1
	F6HHG2	60S Ribosomal protein L1p/L10e family	144.76	7.18	GSVIVT01036128001	AT5G22440.1
	F6HJL1	Class-II DAHP synthetase family protein	144.23	7.17	GSVIVT01006634001	AT1G22410.1
	D7TIY1	Threonine dehydratase	144.20	7.17	GSVIVT01033731001	AT3G10050.1
	D7SGV3	Adenylate kinase 1	143.18	7.16	GSVIVT01008505001	AT5G63400.1
	F6H9P9	Acetyl Co-enzyme a carboxylase biotin carboxylase subunit	142.02	7.15	GSVIVT01032257001	AT5G35360.1
	F6HTU0	non-ATPase subunit 9	141.42	7.14	GSVIVT01021852001	AT1G29150.1
	A5BIN1	UDP-Xylose synthase 6	141.19	7.14	GSVIVT01016574001	AT2G28760.1
	F6HF82	UDP-glucose 6-dehydrogenase family protein	140.06	7.13	GSVIVT01012198001	AT5G15490.1

	F6GY71	Pyruvate decarboxylase-2	139.10	7.12	GSVIVT01003940001	AT5G54960.1
	D7SNX7	Regulatory particle non-ATPase 10	138.44	7.11	GSVIVT01018756001	AT4G38630.1
	D7STV9	Ribosomal protein S3 family protein	137.04	7.10	GSVIVT01035451001	AT5G35530.1
	F6H2N7	Phosphoenolpyruvate carboxylase 3	135.81	7.09	GSVIVT01014206001	AT3G14940.1
	D7UAC9	DEAD box RNA helicase (RH3)	135.38	7.08	GSVIVT01031360001	AT5G26742.2
	F6I0F6	Alcohol dehydrogenase 1	135.29	7.08	GSVIVT01026507001	AT1G77120.1
	D7TXR6	Basic transcription factor 3	134.66	7.07	GSVIVT01029373001	AT1G17880.1
	A5B2Z7	Pyruvate dehydrogenase complex E1 alpha subunit	133.32	7.06	GSVIVT01020139001	AT1G59900.1
	A5B8K7	Mercaptopyruvate sulfurtransferase 1	132.78	7.05	GSVIVT01036786001	AT1G79230.1
	F6HFN8	Dihydrolipoamide acetyltransferase component of pyruvate dehydrogenase complex	132.46	7.05	GSVIVT01034492001	AT3G25860.1
	A5AXI5	20S proteasome alpha subunit G1	132.30	7.05	GSVIVT01025839001	AT2G27020.1
	F6HPH1	Glutathione S-transferase family protein	130.87	7.03	GSVIVT01020103001	AT1G10370.1
	A5B3K9	40S ribosomal protein S13A	130.82	7.03	GSVIVT01027637001	AT4G00100.1
	F6GX19	Isopentenyl pyrophosphate:dimethylallyl pyrophosphate isomerase 2	128.64	7.01	GSVIVT01019089001	AT3G02780.1
	D7TPP7	Phragmoplast orienting kinesin 2	128.44	7.00	GSVIVT01031809001	AT3G19050.1
	F6HQ88	Poly(A) binding protein 2	127.23	6.99	GSVIVT01031709001	AT4G34110.1
	D7UA89	ATP-citrate lyase A-3	126.76	6.99	GSVIVT01031310001	AT1G09430.1
	F6H5T1	Phosphoribosyl formylglycinamidine cyclo-ligase. chloroplastic	121.43	6.92	GSVIVT01028086001	AT3G55010.2
	D7SRG7	Metallopeptidase M24 family protein	121.33	6.92	GSVIVT01003934001	AT3G51800.3
	A5AKA8	Eukaryotic translation initiation factor 2 gamma subunit	120.55	6.91	GSVIVT01034691001	AT1G04170.1
	F6H0C8	TCP-1/cpn60 chaperonin family protein	120.37	6.91	GSVIVT01008708001	AT5G20890.1
	A5B0X9	Delta-aminolevulinic acid dehydratase	118.82	6.89	GSVIVT01008851001	AT1G69740.1
	A5AXR4	UDP-Xylose synthase 6	118.75	6.89	GSVIVT01025003001	AT2G28760.3
	D7UAV2	4-hydroxy-4-methyl-2-oxoglutarate aldolase	116.47	6.86	GSVIVT01014857001	AT5G56260.1
	F6I6W5	Pyrophosphate--fructose 6-phosphate 1-phosphotransferase subunit alpha	115.88	6.86	GSVIVT01013442001	AT1G20950.1
	F6HNI3	60S Ribosomal protein L10 family protein	112.41	6.81	GSVIVT01016313001	AT2G40010.1
	D7SW76	Copper ion binding;cobalt ion binding;zinc ion binding	112.15	6.81	GSVIVT01022249001	AT2G21870.1

	F6HDW1	Pyruvate kinase family protein	110.99	6.79	GSVIVT01018079001	AT3G22960.1
	A5AEB9	AAA-type ATPase family protein	110.63	6.79	GSVIVT01009774001	AT1G45000.1
	A5AL04	Eukaryotic translation initiation factor 3 subunit	110.04	6.78	GSVIVT01011562001	AT2G46290.1
	F6GUF4	10-formyltetrahydrofolate synthetase	109.64	6.78	GSVIVT01025376001	AT1G50480.1
	D7TVK9	Regulatory particle non-ATPase 12A	109.21	6.77	GSVIVT01019594001	AT1G64520.1
	D7SNV6	3-dehydroquinate synthase. putative	108.86	6.77	GSVIVT01018732001	AT5G66120.2
	Q84U32	Putative serine/threonine kinase/ Calcium-binding EF-hand family protein	105.74	6.72	GSVIVT01004914001	AT1G12310.1
	F6GU75	Regulatory particle triple-A ATPase 3	105.21	6.72	GSVIVT01024544001	AT5G58290.1
	D7SLU3	T-complex protein 1 alpha subunit	105.17	6.72	GSVIVT01018213001	AT3G20050.1
	F6H9U0	Inosine-5'-monophosphate dehydrogenase	103.01	6.69	GSVIVT01036725001	AT1G16350.1
	D7T043	isopropylmalate dehydrogenase 2	102.65	6.68	GSVIVT01023010001	AT1G80560.1
	D7TIZ5	Pyruvate kinase family protein	101.54	6.67	GSVIVT01033747001	AT3G52990.1
	F6HGH6	cell elongation protein	101.41	6.66	GSVIVT01010184001	AT3G19820.3
	A5BR49	Translation initiation factor IF6	100.11	6.65	GSVIVT01022313001	AT3G55620.1
	D7TT48	TCP-1/cpn60 chaperonin family protein	99.49	6.64	GSVIVT01031067001	AT3G02530.1
	D7TAR8	Proteasome subunit beta	97.73	6.61	GSVIVT01010375001	AT3G26340.1
	F6HNV2	Rubisco activase	97.23	6.60	GSVIVT01016501001	AT2G39730.2
	E0CV92	Major facilitator superfamily protein	95.79	6.58	GSVIVT01038605001	AT4G27720.1
	D7TKJ3	Ferredoxin--NADP reductase/ root FNR 2	93.25	6.54	GSVIVT01021650001	AT1G30510.1
	Q0ZJ03	Cytochrome b559 subunit alpha / photosystem II reaction center protein B	90.07	6.49		ATCG00680.1
	D7TJ45	60S acidic ribosomal protein family	84.51	6.40	GSVIVT01033814001	AT3G44590.1
	D7SS06	Vacuolar ATP synthase subunit A	81.79	6.35	GSVIVT01029546001	AT1G78900.1
	F6HNE4	P-loop containing nucleoside triphosphate hydrolases superfamily protein	80.92	6.34	GSVIVT01016242001	AT3G10350.1
	D7SM51	NAD-dependent malic enzyme 1	79.44	6.31	GSVIVT01018377001	AT2G13560.1
	A5BXT5	Guanosine nucleotide diphosphate dissociation inhibitor	77.92	6.28	GSVIVT01038268001	AT3G59920.1
	D7SY66	Importin alpha isoform 1	77.18	6.27	GSVIVT01035047001	AT3G06720.2
	B6VJV5	NADH dehydrogenase subunit 9/ Heavy metal transport	74.96	6.23	GSVIVT01011777001	AT1G23000.1
	D7TVX4	Peptidase M1 family protein	74.15	6.21	GSVIVT01019730001	AT1G63770.5

	F6H9H8	UDP-glucose 4.6-dehydratase /rhamnose biosynthesis	73.33	6.20	GSVIVT01033176001	AT1G78570.1
	D7UA22	Inorganic H pyrophosphatase family protein	73.11	6.19	GSVIVT01031230001	AT1G15690.1
	F6HUQ8	6-phosphogluconate dehydrogenase decarboxylating	70.55	6.14	GSVIVT01019467001	AT3G59140.1
	D7SVE1	Tudor-SN protein 1	69.42	6.12	GSVIVT01032946001	AT5G07350.1
	F6HHX2	Transducin/WD40 repeat-like superfamily protein	69.40	6.12	GSVIVT01001441001	AT1G18830.1
	F6H5M5	Casein lytic proteinase B3	68.48	6.10	GSVIVT01011496001	AT5G15450.1
	F6HHF5	Eukaryotic initiation factor 4A-III	66.61	6.06	GSVIVT01036113001	AT3G19760.1
	D7TM20	Lactate/malate dehydrogenase family protein	65.34	6.03	GSVIVT01016172001	AT5G58330.2
	A5ACP0	Clathrin. heavy chain	65.20	6.03	GSVIVT01032792001	AT3G11130.1
	F6GTP5	Alpha-mannosidase/ Glycosyl hydrolase family 38 protein	64.49	6.01	GSVIVT01008340001	AT5G13980.1
	F6HHQ7	Thiolase family protein	62.77	5.97	GSVIVT01030112001	AT5G47720.4
	D7TLU7	Triosephosphate isomerase	62.53	5.97	GSVIVT01016559001	AT3G55440.1
	A5BIQ8	40S Ribosomal protein S5 family protein	62.28	5.96	GSVIVT01033299001	AT3G57490.1
	D7SHS1	1-deoxy-D-xylulose 5-phosphate reductoisomerase	62.15	5.96	GSVIVT01007752001	AT5G62790.1
	F6HQJ5	4-hydroxy-3-methylbut-2-enyl diphosphate reductase	61.24	5.94	GSVIVT01031908001	AT4G34350.1
	F6I4L4	Lysyl-tRNA synthetase 1	61.13	5.93	GSVIVT01031124001	AT3G11710.1
	D7U0U9	Regulatory particle triple-A ATPase 6A	60.20	5.91	GSVIVT01017222001	AT5G19990.1
	D7SJV3	Clathrin. heavy chain	59.96	5.91	GSVIVT01024708001	AT3G11130.1
	D7U0U7	Transducin/WD40 repeat-like superfamily protein	59.85	5.90	GSVIVT01017219001	AT3G15610.1
	F6HK75	SNF1-related protein kinase 2.10	59.17	5.89	GSVIVT01023339001	AT1G60940.2
	F6GZK4	Serine hydroxymethyltransferase 2	57.52	5.85	GSVIVT01009226001	AT5G26780.1
	F6H116	Glucose-6-phosphate isomerase/ phosphoglucose isomerase 1	56.64	5.82	GSVIVT01009147001	AT4G24620.1
	D7SHK5	P-loop containing nucleoside triphosphate hydrolases superfamily protein	56.02	5.81	GSVIVT01007665001	AT5G63120.1
	D7TAP7	NAD(P)-binding Rossmann-fold superfamily protein	55.22	5.79	GSVIVT01010352001	AT1G24360.1
	F6H6Y0	Multifunctional protein 2	54.77	5.78	GSVIVT01035128001	AT3G06860.1
	F6I3Y5	Eukaryotic release factor 1-3	52.61	5.72	GSVIVT01009682001	AT3G26618.1
	F6HLF4	P-loop containing nucleoside triphosphate hydrolases superfamily protein	46.85	5.55	GSVIVT01033437001	AT3G58570.1
	D7TTF4	Dynamin-like 1E	44.07	5.46	GSVIVT01013218001	AT3G60190.1

	D7TQ06	Coatomer gamma-2 subunit. putative	41.64	5.38	GSVIVT01031955001	AT4G34450.1
	F6HN88	2-oxoglutarate dehydrogenase. E1 component	41.38	5.37	GSVIVT01016597001	AT3G55410.1
	F6H710	Mevalonate/galactokinase family protein	39.72	5.31	GSVIVT01034964001	AT3G06580.1
	A3FA66	Aquaporin PIP14/plasma membrane intrinsic protein 1C	35.97	5.17	GSVIVT01019743001	AT1G01620.1
	A5BVN4	Nucleoside diphosphate kinase family protein	22.44	4.49	GSVIVT01019539001	AT4G23900.1
	E0CQR2	Starch branching enzyme	6.42	2.68	GSVIVT01008673001	AT5G03650.1
	F6HNX5	Heat shock protein 70 (Hsp 70) family protein	4.50	2.17	GSVIVT01038580001	AT5G42020.1
Stage	**Uniprot ID**	**Description**	**EM/ON**	**log2**	**Phytozome DB *V. vinifera***	**Orthologous gene *A.thaliana***
Ripe Higher in EM	D7SUD7	Aspartate aminotransferase, cytoplasmic	849.83	9.73	GSVIVT01035662001	AT5G11520.1
	A5B605	Translation initiation factor 5A	558.96	9.13	GSVIVT01007954001	AT1G13950.1
	F6HTH5	Triose-phosphate isomerase	437.38	8.77	GSVIVT01015656001	AT3G55440.1
	F6GTE2	UDP-arabinopyranose mutase	401.78	8.65	GSVIVT01008552001	AT3G02230.1
	F6GUQ0	Ran-binding protein 1	397.35	8.63	GSVIVT01024705001	AT5G58590.1
	F6HCT7	Molecular chaperone DnaK	387.58	8.60	GSVIVT01038517001	AT5G09590.1
	D7TUX2	Shikimate-NADP(+) oxidoreductase	362.64	8.50	GSVIVT01021978001	AT3G06350.1
	F6HW56	Molecular chaperone DnaK	362.26	8.50	GSVIVT01038517001	AT5G09590.1
	D7TE88	Multi cooper oxidase	307.68	8.27	GSVIVT01030441001	AT1G76160.1
	D7TUP8	Cysteine synthase	302.01	8.24	GSVIVT01021874001	AT4G14880.3
	A5C4U9	Light-harvesting complex II chlorophyll a/b binding protein	290.56	8.18	GSVIVT01014439001	AT5G54270.1
	D7TRL3	Small subunit ribosomal protein	288.32	8.17	GSVIVT01003418001	AT5G10360.1
	F6I4L5	Mediator of RNA polymerase transcription subunit related	279.02	8.12	GSVIVT01031125001	AT5G42020.2
	D7TQA5	L-Ascorbate peroxidase, cytosolic	266.69	8.06	GSVIVT01025551001	AT3G09640.1
	F6I019	Large subunit ribosomal protein L13	263.07	8.04	GSVIVT01028661001	AT3G24830.1
	E0CR63	Photosystem II 22kDa protein	256.13	8.00	GSVIVT01008866001	AT1G44575.1
	D7T9L8	Coatomer subunit delta	237.19	7.89	GSVIVT01012108001	AT5G05010.1
	F6HXY7	ATP-dependent RNA helicase	233.34	7.87	GSVIVT01016795001	AT5G11200.1

	F6HFL6	Fructose bisphosphate aldolase 3, chloroplastic- related	220.08	7.78	GSVIVT01011810001	AT2G01140.1
	D7TLU7	Large subunit ribosomal protein L9	218.32	7.77	GSVIVT01016559001	AT4G10450.1
	A5ALT5	DnaJ homolog subfamily A member 2	213.35	7.74	GSVIVT01036049001	AT5G22060.1
	F6HLL3	Large subunit ribosomal protein L6e	203.88	7.67	GSVIVT01033532001	AT1G74050.1
	D7UC26	Malate dehydrogenase (decarboxylating) / Pyruvic-malic carboxylase	191.87	7.58	GSVIVT01026824001	AT4G00570.1
	F6I120	Amidase	186.49	7.54	GSVIVT01024064001	AT4G34880.1
	F6H7H1	Aspartic proteinase A1 related	177.79	7.47	GSVIVT01012684001	AT1G11910.1
	F6H2E4	Chlorophyll a-b binding protein, chloroplastic	169.71	7.41	GSVIVT01014439001	AT3G43190.1
	D7U704	RAS-related protein	167.06	7.38	GSVIVT01004643001	AT4G17170.1
	F6H9U0	Inosinic acid dehydrogenase	160.86	7.33	GSVIVT01036725001	AT1G16350.1
	F6H9H8	UDP-glucose 4,6-dehydratase /rhamnose biosynthesis	156.32	7.29	GSVIVT01033176001	AT1G78570.1
	D7TKA5	Ornithine aminotransferase	152.81	7.26	GSVIVT01021525001	AT5G46180.1
	D7TVX5	Aminopeptidase	150.38	7.23	GSVIVT01019731001	AT1G63770.5
	F6GUR4	Pyridoxal 5'-phosphate synthase pdxS subunit	136.82	7.10	GSVIVT01024735001	AT5G01410.1
	D7TQ10	Adenylyl cyclase-associated protein	135.80	7.09	GSVIVT01031961001	AT4G34490.1
	F6GUF4	Tetrahydrofolic formylase	133.87	7.06	GSVIVT01025376001	AT1G50480.1
	A5C319	Protien phosphatase 2C 20-related	130.33	7.03	GSVIVT01020581001	AT4G28400.1
	F6HMP3	3-isopropylmalate/(R)-2-methylmalate dehydratase large subunit	124.13	6.96	GSVIVT01029978001	AT4G13430.1
	D7TDB5	Ras-related protein Rab-2A	121.09	6.92	GSVIVT01030140001	AT4G17170.1
	F6HAM6	ubiquinol-cytochrome c reductase cytochrome b subunit	120.21	6.91	GSVIVT01018555001	AT2G07727.1
	F6HDW4	Malate dehydrogenase (decarboxylating) / Pyruvic-malic carboxylase	119.91	6.91	GSVIVT01018081001	AT2G13560.1
	D7TR81	Pyrophosphate--fructose 6-phosphate 1-phosphotransferase subunit beta	117.23	6.87	GSVIVT01004820001	AT1G12000.1
	A5AXI5	Proteasome subunit alpha 7	115.67	6.85	GSVIVT01025839001	AT2G27020.1
	D7SVZ9	Myo-inositol-1-phosphate synthase	112.73	6.82	GSVIVT01022158001	AT2G22240.1
	A5AKV9	Aspartyl protease related	108.78	6.77	GSVIVT01027158001	AT1G01300.1
	F6HGF1	Heat shock protein 90kDa beta	108.49	6.76	GSVIVT01010120001	AT2G04030.1
	Q0ZIY9	Di-haem cytochrome. transmembrane; Cytochrome b/b6. C-terminal	107.17	6.74	GSVIVT01018702001	AT2G07727.1
	D7TIZ1	Large subunit ribosomal protein L24e	105.75	6.72	GSVIVT01033743001	AT2G36620.1

	F6HSN5	2-hydroxyacyl-CoA lyase	104.47	6.71	GSVIVT01030948001	AT5G17380.1
	D7SRG7	Proliferation associated protein 2G4	103.45	6.69	GSVIVT01003934001	AT3G51800.3
	F6HPC4	Methyl transferase PMT2-related	102.35	6.68	GSVIVT01019997001	AT1G26850.2
	D7U8V6	Tyrosine protein kinase related	96.69	6.60	GSVIVT01013564001	AT3G59350.3
	F6HBC7	Sterol 24-C-methyltransferase	92.63	6.53	GSVIVT01032155001	AT5G13710.1
	D7TBJ2	Rab GDP dissociation inhibitor	87.74	6.46	GSVIVT01015339001	AT5G09550.1
	D7TAP7	3-oxoacyl- (fabG)	85.64	6.42	GSVIVT01010352001	AT1G24360.1
	F6HJ88	Xyloglucan endotransglucosylase/ hydrolase protein	85.50	6.42	GSVIVT01001124001	AT5G13870.1
	D7T6C5	Plastidial pyruvate kinase, chloroplastic	83.30	6.38	GSVIVT01017724001	AT3G22960.1
	D7TXR6	Nascent polypeptide-associated complex subunit beta	78.93	6.30	GSVIVT01029373001	AT1G17880.1
	D7UA89	ATP- citrate synthase / Citric cleavage enzyme	78.59	6.30	GSVIVT01031310001	AT1G09430.1
	F6HSN0	NADH dehydrogenase (ubiquinone) Fe-S protein 1	73.84	6.21	GSVIVT01030914001	AT5G37510.2
	F6H316	26S proteasome regulatory subunit T5	73.21	6.19	GSVIVT01017308001	AT3G05530.1
	D7SM51	Transketolase / Glycoaldehyde transferase	73.10	6.19	GSVIVT01018377001	AT2G45290.1
	F6HGZ9	Lacto glutathione lyase- glyoxalase	72.18	6.17	GSVIVT01015018001	AT1G67280.1
	F6GX19	Isopentenyl-diphosphate delta-isomerase	69.91	6.13	GSVIVT01019089001	AT3G02780.1
	F6H0B6	ATP-Dependent zinc metalloprotease, chloroplastic related	66.95	6.07	GSVIVT01008686001	AT1G50250.1
	D7TQG4	Inorganic pyrophosphatase like protein	66.28	6.05	GSVIVT01025621001	AT3G53620.1
	F6HLF4	ATP-dependent RNA helicase	63.24	5.98	GSVIVT01033437001	AT3G58570.1
	F6HEJ3	Polyadenylate binding protein RBP45B-related	62.48	5.97	GSVIVT01025280001	AT5G19350.1
	A5C0T5	Large subunit ribosomal protein L21e	62.20	5.96	GSVIVT01033455001	AT1G09590.1
	F6HHQ7	Acetyl-CoA C-acetyltransferase	61.97	5.95	GSVIVT01030112001	AT5G47720.4
	D7SLA9	Lipoxygenase	59.47	5.89	GSVIVT01025339001	AT3G45140.1
	E0CV92	Sugar-transporters	59.44	5.89	GSVIVT01038605001	AT4G27720.1
	D7SV44	Transmembrane 9 superfamily member	58.38	5.87	GSVIVT01035970001	AT5G25100.1
	F6HJZ9	Cullin-associated NEDD8-dissociated protein	55.51	5.79	GSVIVT01023143001	AT2G02560.2
	F6GUS0	Pur-transcriptional activator	54.68	5.77	GSVIVT01025513001	AT2G32080.2
	E0CUM8	Plastidial pyruvate kinase	51.80	5.69	GSVIVT01028756001	AT5G52920.1

	F6H6C3	Molecular chaperone HtpG	51.23	5.68	GSVIVT01028856001	AT5G56010.1
	D7SNS5	Selenium-binding protein 1	51.00	5.67	GSVIVT01021049001	AT4G14030.2
	F6GSS9	Malate synthase / Malic-condensing enzyme	50.57	5.66	GSVIVT01008494001	AT5G03860.2
	F6HDW1	GDP-mannose 3,5-epimerase	49.91	5.64	GSVIVT01018079001	AT5G28840.2
	A5AL04	Translation initiation factor 3 subunit I	49.59	5.63	GSVIVT01011562001	AT2G46290.1
	F6HQ88	Polyadenylate-binding protein	47.83	5.58	GSVIVT01031709001	AT4G34110.1
	A5C6V1	26S proteasome regulatory subunit N11	45.84	5.52	GSVIVT01009529001	AT5G23540.1
	D7SVD4	Acetyl-CoA synthetase	42.57	5.41	GSVIVT01032938001	AT5G36880.2
	D7SZH8	Methyl transferase PMT1-related	41.77	5.38	GSVIVT01027829001	AT1G04430.1
	F6GST3	Argininosuccinate synthase	39.36	5.30	GSVIVT01008510001	AT4G24830.1
	D7TWZ7	Mannose-1-phosphate guanylyltransferase	24.15	4.59	GSVIVT01032587001	AT1G74910.1
	D7TCR2	Nicastrin	21.37	4.42	GSVIVT01036081001	AT3G44330.1
	F6HQT9	Eukariotic translation initiation factor 2C	15.33	3.94	GSVIVT01025868001	AT2G27040.2
Stage	**Uniprot ID**	**Description**	**EM/ON**	**Log2**	**Phytozome DB *V.vinifera***	**Orthologous gen *A. thaliana***
Fruit set Higher in ON	E0CU14	Glutathione S-Transferase	0.0009	-10.10	GSVIVT01020831001	AT2G30860.1
	E0CR49	Protein disulphide isomerase	0.0022	-8.86	GSVIVT01008848001	AT1G21750.1
	F6GTA6	Hypersensitive- induced response protein	0.0026	-8.59	GSVIVT01008060001	AT5G62740.1
	D7TKA1	Peroxisomal-2-hydroxyacid oxidase	0.0026	-8.56	GSVIVT01021520001	AT3G14420.1
	F6H409	Glyceraldehyde-3-phosphate dehydrogenase (phosphorylating) (NADP+)	0.0028	-8.47	GSVIVT01032942001	AT1G12900.1
	A5BTZ8	Annexin D1-related	0.0033	-8.26	GSVIVT01009021001	AT5G65020.1
	D7TNE5	Band 7 protein-related	0.0034	-8.20	GSVIVT01020071001	AT5G62740.1
	A5BX41	Plastoquinol-plastocyanin reductase / Cytochrome b6f complex	0.0038	-8.03	GSVIVT01014457001	AT4G03280.1
	D7SIH5	ATPase 11. plasma membrane	0.0043	-7.88	GSVIVT01008074001	AT5G62670.1
	D7SZH4	Aryl alcohol dehydrogenase related	0.0044	-7.81	GSVIVT01027822001	AT1G04420.1
	D7U7L6	Abieta-7.13-dien-18-ol hydroxylase	0.0046	-7.77	GSVIVT01027541001	AT2G45510.1
	A5C6H7	Sucrose synthase 2	0.0048	-7.71	GSVIVT01028043001	AT4G02280.1

	F6I5Y5	2-hydroxyacid dehydrogenase related	0.0050	-7.65	GSVIVT01009428001	AT4G34200.1
	E0CQN2	Alcohol dehydrogenase related	0.0050	-7.63	GSVIVT01010024001	AT1G77120.1
	D7SKK6	RAS-related protein	0.0059	-7.40	GSVIVT01025028001	AT5G59840.1
	D7SHU4	Phenylacetaldehyde dehydrogenase	0.0066	-7.24	GSVIVT01007784001	AT3G48000.1
	D7TT84	Formamide amidohydrolase	0.0072	-7.12	GSVIVT01000135001	AT4G37560.1
	F6HGZ1	Pectinmethylesterase	0.0077	-7.02	GSVIVT01014999001	AT3G14310.1
	F6HGX0	Asparaginyl-tRNA synthetase	0.0164	-5.93	GSVIVT01015254001	AT5G56680.1
	F6I1W0	Glutamate decarboxylase	0.0176	-5.83	GSVIVT01000391001	AT5G17330.1
Stage	**Uniprot ID**	**Description**	**EM/ON**	**Log2**	**Phytozome DB *V.vinifera***	**Orthologous gene *A. thaliana***
Ripe Higher in ON	F6H5F0	ADP/ATP carrier 2	0.0004	-11.24	GSVIVT01025296001	AT5G13490.2
	F6GZC5	Basic chitinase	0.0011	-9.85	GSVIVT01007190001	AT3G12500.1
	A5BPB2	Light-harvesting chlorophyll B-binding protein 3	0.0019	-9.03	GSVIVT01014439001	AT5G54270.1
	F6HV69	Aldehyde dehydrogenase 10A8	0.0019	-9.01	GSVIVT01032588001	AT1G74920.1
	F6I1W0	Glutamate decarboxylase	0.0031	-8.34	GSVIVT01000391001	AT5G17330.1
	D7SQD1	H(+)-ATPase 2	0.0042	-7.89	GSVIVT01029244001	AT4G30190.1
	F6GZD1	Elicitor-activated gene 3-2	0.0042	-7.89	GSVIVT01002106001	AT4G37990.1
	F6H344	Glutathione peroxidase 1	0.0043	-7.86	GSVIVT01035981001	AT2G25080.1
	F6H3Q4	17.6 kDa class II heat shock protein	0.0045	-7.81	GSVIVT01035430001	AT5G12020.1
	F6HAR3	Cytochrome P450. family 704. subfamily A. polypeptide 2	0.0048	-7.71	GSVIVT01018473001	AT2G45510.1
	D7SNA2	Copper/zinc superoxide dismutase 2	0.0048	-7.70	GSVIVT01031462001	AT2G28190.1
	D7UDM2	Vesicle-associated membrane protein 726	0.0054	-7.53	GSVIVT01000524001	AT1G04760.1
	A5C4J2	Ribosomal protein S19e family protein	0.0055	-7.52	GSVIVT01007908001	AT5G61170.1
	D7SKV8	Isovaleryl-CoA-dehydrogenase	0.0070	-7.17	GSVIVT01025158001	AT3G45300.1
	Q0ZJ21	Photosystem I. PsaA/PsaB protein	0.0071	-7.13	GSVIVT01017483001	ATCG00340.1
	F6GZU4	RAB GTPase homolog B18	0.0074	-7.08	GSVIVT01009987001	AT1G43890.2

	D7U0V9	Cytochrome C1 family	0.0075	-7.05	GSVIVT01017236001	AT5G40810.1
	F6GVX0	Light harvesting complex of photosystem II 5	0.0076	-7.03	GSVIVT01037111001	AT4G10340.1
	F6GV40	Histone superfamily protein	0.0078	-7.00	GSVIVT01025025001	AT5G59910.1
	F6H1U2	Target of Myb protein 1	0.0080	-6.96	GSVIVT01014122001	AT5G16880.1
	F6HAB0	Glycosyl hydrolase family protein	0.0084	-6.90	GSVIVT01022483001	AT5G20950.1
	D7U851	Prohibitin 1	0.0087	-6.85	GSVIVT01027465001	AT4G28510.1
	F6H2W4	Class II aminoacyl-tRNA and biotin synthetases superfamily protein	0.0089	-6.81	GSVIVT01035583001	AT4G31180.1
	D7SYK8	ATP citrate lyase subunit B 2	0.0092	-6.76	GSVIVT01034990001	AT5G49460.1
	F6GUE3	NAD(P)-binding Rossmann-fold superfamily protein	0.0098	-6.68	GSVIVT01025358001	AT2G05990.1
	F6HF38	Alanyl-tRNA synthetase	0.0103	-6.61	GSVIVT01024320001	AT1G50200.1
	F6HG55	Adenylate kinase 1	0.0114	-6.45	GSVIVT01010361001	AT5G63400.1
	F6HBE7	Protein of unknown function (DUF3411)	0.0119	-6.39	GSVIVT01032197001	AT5G12470.1
	D7UDC9	Glyceraldehyde-3-phosphate dehydrogenase B subunit	0.0129	-6.27	GSVIVT01013403001	AT1G42970.1
	F6HFN8	2-oxoacid dehydrogenases acyltransferase family protein	0.0134	-6.22	GSVIVT01034492001	AT3G25860.1
	D7SRB4	Fructose-1.6-bisphophatase	0.0138	-6.18	GSVIVT01034516001	AT1G43670.1
	D7U0U7	Transducin/WD40 repeat-like superfamily protein	0.0172	-5.86	GSVIVT01017219001	AT3G15610.1
	F6H9P9	Acetyl Co-enzyme a carboxylase biotin carboxylase subunit	0.0202	-5.63	GSVIVT01032257001	AT5G35360.1
	F6I1U3	Dynamin-related protein 3A	0.0209	-5.58	GSVIVT01012532001	AT4G33650.1
	F6HHF5	Eukaryotic initiation factor 4A-III	0.0407	-4.62	GSVIVT01036113001	AT3G19760.1

Highlights

- Metabolite and protein content are related with quality attributes of blueberries.
- Divergences were found between processes at two phenological stages for each variety.
- During fruit set, the firmer variety efficiently manage C:N balance and water resources.
- Ripe Emerald fruit has increased cell wall recycling, inositol and phenolic content.
- The cell wall calcium content does not vary significantly between varieties.